A Synthetic Analogue of the Active Site of Fe-Containing Nitrile Hydratase with Carboxamido N and Thiolato S as Donors: Synthesis, Structure, and Reactivities

Juan C. Noveron, Marilyn M. Olmstead, and Pradip K. Mascharak*

Contribution from the Department of Chemistry and Biochemistry, University of California, Santa Cruz, California 95064, and, Department of Chemistry, University of California, Davis, California 95616

Received April 10, 2000. Revised Manuscript Received September 4, 2000

Abstract: As part of our work on models of the iron(III) site of Fe-containing nitrile hydratase, a designed ligand $PyPSH_4$ with two carboxamide and two thiolate donor groups has been synthesized. Reaction of $(Et_4N)[FeCl_4]$ with the deprotonated form of the ligand in DMF affords the mononuclear iron(III) complex $(Et_4N)[Fe^{III}(PyPS)]$ (**1**) in high yield. The iron(III) center is in a trigonal bipyramidal geometry with two deprotonated carboxamido nitrogens, one pyridine nitrogen, and two thiolato sulfurs as donors. Complex **1** is stable in water and binds a variety of Lewis bases at the sixth site at low temperature to afford green solutions with a band around 700 nm. The iron(III) centers in these six-coordinate species are low-spin and exhibit EPR spectra much like the enzyme. The pK_a of the water molecule in $[Fe^{III}(PyPS)(H_2O)]^-$ is 6.3 ± 0.4. The iron(III) site in **1** with ligated carboxamido nitrogens and thiolato sulfurs does not show any affinity toward nitriles. It thus appears that at physiological pH, a metal-bound hydroxide promotes hydration of nitriles nested in close proximity of the iron center in the enzyme. Redox measurements demonstrate that the carboxamido nitrogens prefer Fe(III) to Fe(II) centers. This fact explains the absence of any redox behavior at the iron site in nitrile hydratase. Upon exposure to limited amount of dioxygen, **1** is converted to the bis-sulfinic species. The structure of the more stable O-bonded sulfinato complex $(Et_4N)[Fe^{III}(PyP\{S\underline{O}_2\}_2)]$ (**2**) has been determined. Six-coordinated low-spin cyanide adducts of the S-bonded and the O-bonded sulfinato complexes, namely, $Na_2[Fe^{III}(PyP\{S\underline{O}_2\}_2)(CN)]$ (**4**) and $(Et_4N)_2[Fe^{III}(PyP\{S\underline{O}_2\}_2)(CN)]$ (**5**), afford green solutions in water and other solvents. The iron(II) complex $(Et_4N)_2[Fe^{II}(PyPS)]$ (**3**) has also been isolated and structurally characterized.

Introduction

The microbial enzyme Nitrile Hydratase (NHase) catalyzes the hydrolysis of a wide variety of nitriles (RCN) to the corresponding amides ($RCONH_2$).[1−5] In recent years, NHases from several microorganisms (and related mutants) have been employed as biocatalysts in industrial production of acrylamide in kiloton quantities[6−10] and in enantioselective syntheses of other carboxamides.[11−14] NHases have also been used in environmental remediation of nitriles.[15−17] NHases consist of α and β subunits and exist as $\alpha\beta$ 46 kDa heterodimers or $(\alpha\beta)_2$ 92 kDa tetramers. The α subunit contains either a low-spin ($S = {}^1/_2$) non-heme iron(III) center[18,19] or a non-corrinoid cobalt-(III) center,[20−22] depending on the bacterial source, and these M(III) centers have been shown to be the active site for hydrolysis of nitriles. Unlike other non-heme iron centers in biology,[23,24] the iron(III) center of the NHase does not participate in redox reaction(s) and acts as a Lewis acid. The iron- and cobalt-containing NHases (Fe−NHase and Co−NHase, hereafter) possess almost identical sequence homology at the loci of their active sites, and they hydrolyze nitriles at similar rates. These observations have led to the suggestion that the structures

(1) Endo, I.; Odaka, M.; Yohda, M. *Trends Biotechnol.* **1999**, *17*, 244.
(2) Kobayashi, M.; Shimizu, S. *Nature Biotechnol.* **1998**, *16*, 733.
(3) Hjort, C. M.; Godtfredsen, S. E.; Emborg, C. *J. Chem. Technol. Biotechnol.* **1990**, *48*, 217.
(4) Nagasawa, T.; Yamada, H. *Trends in Biotechnol.* **1989**, *7*, 153.
(5) Nagasawa, T.; Ryuno, K.; Yamada, H. *Biochem. Biophys. Res. Commun.* **1986**, *139*, 1305.
(6) Nagasawa, T.; Ryuno, K.; Yamada, H. *Experientia* **1989**, *45*, 1066.
(7) Kobayashi, M.; Nagasawa, T.; Yamada, H. *Trends Biotechnol.* **1992**, *10*, 402.
(8) Nagasawa, T.; Shimizu, H.; Yamada, H. *Appl. Microbiol. Biotechnol.* **1993**, *40*, 189.
(9) Yamada, H.; Kobayashi, M. *Biosci. Biotechnol. Biochem.* **1996**, *60*, 1391.
(10) Padmakumar, R.; Oriel, P. *Appl. Biochem. Biotechnol.* **1999**, *77*, 671.
(11) Kakeya, H.; Sakai, N.; Sugai, T.; Ohta, H. *Tetrahedron Lett.* **1991**, *32*, 1343.
(12) Stolz, A.; Trott, S.; Binder, M.; Bauer, R.; Hirrlinger, B.; Layh, N.; Knackmuss, H.-J. *J. Mol. Catal. B: Enzym.* **1998**, *5*, 137.
(13) Maddrell, S. J.; Turner, N. J.; Kerridge, A.; Willetts, A. J.; Crosby, J. *Tetrahedron Lett.* **1996**, *37*, 6001.
(14) Bauer, R.; Knackmuss, H. J.; Stolz, A. *Appl. Microbiol. Biotechnol.* **1998**, *49*, 89.
(15) Battistel, E.; Bernardi, A.; Maestri, P. *Biotechnol. Lett.* **1997**, *19*, 131.
(16) Babu, G. R. V.; Chetty, C. S.; Wolfram, J. H.; Chapatwala, K. D. *J. Environ. Sci. Health, Part A: Environ. Sci. Eng.* **1994**, *29*, 1957.
(17) Wyatt, J. M.; Knowles, K. C. *Int. Biodeterior. Biodegrad.* **1995**, *35*, 227.
(18) Sugiura Y.; Kuwahara J.; Nagasawa, T.; Yamada, H. *J. Am. Chem. Soc.* **1987**, *109*, 5848.
(19) Nelson, M. J.; Jin, H.; Turner, I. M., Jr.; Grove, G.; Scarrow, R. C.; Brennan, B. A.; Que L., Jr. *J. Am. Chem. Soc.* **1991**, *113*, 7072.
(20) Brennan, B. A.; Alms, G.; Nelson, M. J.; Durney, L. T.; Scarrow, R. C. *J. Am. Chem. Soc.* **1996**, *118*, 9194.
(21) Nagasawa, T.; Takeuchi, K.; Yamada, H. *Eur. J. Biochem.* **1991**, *196*, 581.
(22) Payne, M. S.; Wu, S.; Fallon, R. D.; Tudor, G.; Stieglitz, B.; Turner, I. M., Jr.; Nelson, M. J. *Biochemistry* **1997**, *36*, 5447.
(23) Que, L., Jr.; Ho, R. Y. N. *Chem. Rev.* **1996**, *96*, 2607.
(24) Feig, A. L.; Lippard, S. J. *Chem. Rev.* **1994**, *94*, 759.

10.1021/ja001253v CCC: $20.00
Published on Web 04/04/2001

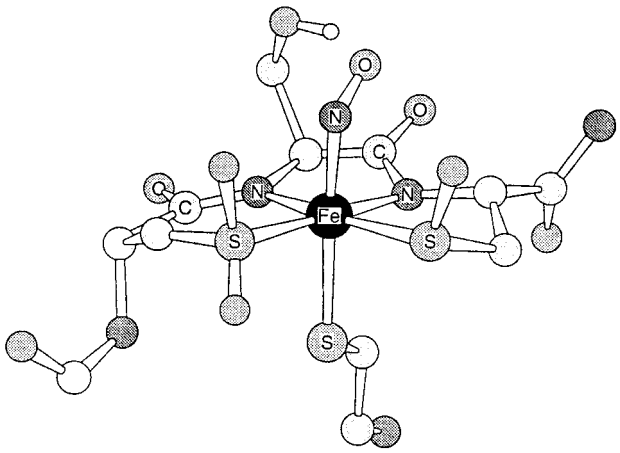

Figure 1. Structure of the NO-bound iron site of *Rhodococcus* sp. N-771 (ref 29).

of the metal sites in the two types of NHases as well as their mode of catalysis are similar in nature. There is, however, an interesting difference between the two varieties of NHases; the activity of the Fe−NHases is regulated by photoreversible binding of exogenous nitric oxide (NO) to the iron center.[25−27] Such a regulatory role of NO in a non-heme iron enzyme is quite unique and is not observed with the Co−NHases.

Recent crystallographic studies on the Fe−NHase from *Rhodococcus* sp. R312 have revealed that the Fe(III) center is ligated to two deprotonated carboxamido nitrogens and three sulfur donors situated in the highly conserved -C-S-L-C-S-C- motif of the α subunit.[28] A more precise (higher resolution) structure of the dark-adapted Fe−NHase isolated from another Rhodococcus species (N771)[29] further reveals that two of the ligated Cys-S residues are posttranslationally modified to the sulfinic(Cys-SO_2) and sulfenic (Cys-SO) forms and a molecule NO is coordinated at the solvent-exposed site of the metal (Figure 1). The iron-bound NO molecule is released upon illumination, and the active form of the NHase is generated.[25−27] The N_2S_3 protein donor set around the iron(III) center is conserved in the active form of the enzyme.[18,19,30−33] Results of spectroscopic studies on the active form of the Fe−NHase from *Rhodococcus* sp. R312 also suggest that a water molecule occupies the site of NO, hence conferring a six-coordinate iron-(III) site with pseudooctahedral geometry. Recent electron−nuclear double resonance (ENDOR) studies[34] however indicate that the iron(III) site may contain a coordinated hydroxide at the optimum pH (pH 7.3) of the enzyme.[34]

The donor set of the iron(III) site of the Fe−NHases, namely, carboxamido N, sulfenato (RSO^-) and sulfinato (RSO_2^-), is unprecedented. Coordination of deprotonated carboxamido N has only been discovered recently in the nitrogenase P cluster[35] while coordination by the modified cysteines residues (RSO^-, RSO_2^-) through the sulfur atoms has not been observed in any other metalloenzyme. Thus far, the mechanism underlying the biogenesis of the modified cysteines remains elusive. Proposed suggestions for such posttranslational modification of cysteines include (a) involvement of oxidative enzymes such as cysteine dioxygenases,[36,37] (b) reaction with peroxynitrite anion derived from NO,[38−40] and (c) generation of iron-peroxides from the reaction between oxygen and the iron center of NHase such as the case with the biogenesis of topa quinone.[41,42] The effect(s) of the modified Cys-S centers on the overall properties of the iron(III) site is an open question in the chemistry of the NHase at this time.

There are several postulated mechanisms for nitrile hydrolysis by NHases.[3,28] The first one involves displacement of the metal-bound water molecule by the nitrile substrate, followed by hydrolysis of the transient metal-bound nitrile species with the eventual rearrangement and release of the amide product (an inner-sphere mechanism). The second mechanism postulates a direct attack of the metal-bound hydroxide on the nitrile group of the substrate with eventual rearrangement to the corresponding amide product (an outer-sphere mechanism). The third mechanism involves activation of a water molecule in close proximity to the metal center via deprotonation by the metal-bound hydroxide. The hydroxide ion generated in such process ultimately causes hydrolysis of nitriles (also an outer-sphere mechanism). To our knowledge, there has not been any report that confirms any one of these mechanisms of nitrile hydrolysis by NHases.

The extent to which the unusual coordination structure of the iron site of the Fe−NHase dictates its ability to hydrolyze nitriles is an important question. To address this question, one needs to determine the intrinsic properties of the iron(III) site via studies on suitably designed model complexes that mimic the coordination structure of the iron(III) center of the Fe−NHases. In such pursuit, Kovacs and co-workers have synthesized a five-coordinated iron(III) complex with N_3S_2 donor set, $[Fe^{III}S_2{}^{Me2}N_3(Pr,Pr)]PF_6$ (structure i), that mimics some features of the active site of the Fe−NHase.[43,44] For example, $[Fe^{III}S_2{}^{Me2}N_3(Pr,Pr)]^+$ reacts with NO to form a diamagnetic photolabile iron−nitrosyl complex. This result is noteworthy since the reactivity of the model complex demonstrates that NO can bind to an iron(III) site and the resultant species could be photolabile. The iron(III) center of $[Fe^{III}S_2{}^{Me2}N_3(Pr,Pr)]^+$ also binds azide (N_3^-), a competetive inhibitor of NHase, in a reversible manner. This model is, however, not a good structural

(25) Noguchi, T.; Honda, J.; Nagamune, T.; Sasabe, H.; Inoune, Y.; Endo, I. *FEBS Lett.* **1995**, *358*, 9.
(26) Noguchi, T.; Hoshino, M.; Tsujimura, M.; Odaka, M.; Inoue, Y.; Endo, I. *Biochemistry* **1996**, *35*, 16777.
(27) Odaka, M.; Fujii, K.; Hoshino, M.; Noguchi, T.; Tsujimura, M.; Nagashima, S.; Yohda, M.; Nagamune, T.; Inoue, Y.; Endo, I. *J. Am. Chem. Soc.* **1997**, *119*, 3785.
(28) Huang, W.; Jia, J.; Cummings, J.; Nelson, M.; Schneider, G.; Lindqvist, Y. *Structure* **1997**, *5*, 691.
(29) Nagashima, S.; Nakasako, M.; Dohmae, N.; Tsujimura, M.; Takio, K.; Odaka, M.; Yohda, M.; Kamiya, N.; Endo, I. *Nat. Struct. Biol.* **1998**, *5*, 347.
(30) Scarrow, R. C.; Brennan, B. A.; Cummings, J. G.; Haiyong, J.; Duong, D. J.; Kindt, J. T.; Nelson, M. J. *Biochemistry* **1996**, *35*, 10078.
(31) Brennan, B. A.; Cummings, J. G.; Chase, B.; Turner, I. M., Jr.; Nelson, M. J. *Biochemistry* **1996**, *35*, 10068.
(32) Jin, H.; Turner, I. M., Jr.; Nelson, M. J.; Gurbiel, R. J.; Doan, P. E.; Hoffman, B. M. *J. Am. Chem. Soc.* **1993**, *115*, 5290.
(33) Scarrow, R. C.; Strickler, B. S.; Ellison, J. J.; Shoner, S. C.; Kovacs, J. A.; Cummings, J. G.; Nelson, M. J. *J. Am. Chem. Soc.* **1998**, *120*, 9237.
(34) Doan, P. E.; Nelson, M. J.; Jin, H.; Hoffman, B. M. *J. Am. Chem. Soc*. **1996**, *118*, 7014.
(35) Peters, J. W.; Stowell, M. H. B.; Soltis, S. M.; Finnegan, M. G.; Johnson, M. K.; Rees, D. C. *Biochemistry* **1997**, *36*, 1181.
(36) Hosokawa, Y.; Matsumoto, A.; Oka, J.; Itakura, H.; Yamaguchi, K. *Biochem. Biophys. Res. Commun.* **1990**, *168*, 473.
(37) McCann, K. P.; Akbari, M. T.; William, A. C.; Ramsden, D. B. *Biochim. Biophys. Acta* **1994**, *1209*, 107.
(38) Radi, R.; Bechman, J. S.; Bush, K. M.; Freeman, B. A. *J. Biol. Chem.* **1991**, *272*, 19157.
(39) Ischiropoulos, H.; Al-Mehdi, A. B. *FEBS Lett*. **1995**, *364*, 279.
(40) DeMaster, E. G.; Quast, B. J.; Redfern, B.; Nagasawa, H. T. *Biochemistry* **1995**, *34*, 11494.
(41) Nakamura, N.; Matsuzaki, R.; Choi, Y. H.; Tanizawa, K.; Sanders-Loehr, J. *J. Biol. Chem.* **1996**, *271*, 4718.
(42) Cai, D.; Klinman, J. P. *Biochemistry* **1994**, *33*, 7647.
(43) Ellison, J. J.; Nienstedt, A.; Shoner, S. C.; Barnhart, D.; Cowen, J. A.; Kovacs, J. A. *J. Am. Chem. Soc.* **1998**, *120*, 5691.
(44) Shweitzer, D.; Ellison, J. J.; Shoner, S. C.; Lovell, S.; Kovacs, J. A. *J. Am. Chem. Soc.* **1998**, *120*, 10996.

mimic since it does not contain any deprotonated carboxamido N in the coordination sphere of iron. Very recently, Chottard and co-workers have reported an iron(III) complex that contains two carboxamido N and three thiolato S donor sets.[45] In this

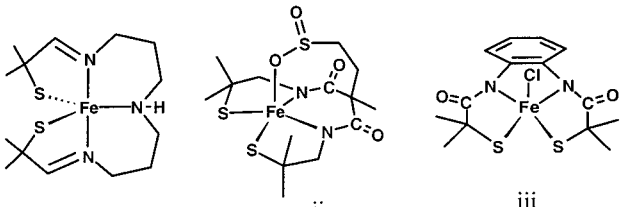

i ii iii

model complex ($(Et_4N)_2[Fe^{III}(L\text{-}O_2)]$, structure ii), one of the thiolato S donors is in the sulfinic form and is bonded to iron through one of the oxygen atoms of the $-SO_2$ unit. Although this model is a very close structural analogue of the iron site in Fe−NHase, its physical parameters ($S = {}^3/_2$ and $\lambda_{max} = 425$ nm) are quite different from those of the iron site of the enzyme ($S = {}^1/_2$, $\lambda_{max} = 700$ nm). This is surprising in view of the structural similarities that exist between the biological iron(III) site and this model complex. In a recent article, Artaud and co-workers have reported an iron(III) complex $(Et_4N)_2[Fe^{III}(N_2S_2)Cl]$ (structure iii) which contains two carboxamido N and two thiolato S donors around the iron center.[46] The spectroscopic parameters for this model complex ($S = {}^3/_2$, $\lambda_{max} = 470$ nm) are also very different from those of Fe−NHase. Clearly, more model studies are required to establish the underlying principles that correlate the structural features with spectroscopic parameters and reactivities.

For some time, we have been involved in syntheses of model complexes that mimic the structural features of the Fe− and Co−NHases.[47−51] In such pursuit, we have reported for the first time the synthesis, structure, and redox properties of iron(III) and cobalt(III) complexes with ligands containing carboxamido N and thiolato S donors.[48,50] The redox properties of the low-spin ($S = {}^1/_2$) complex $(Et_4N)[Fe^{III}(PyPepS)_2]$[48] (structure iv) demonstrate that ligation of carboxamido N to iron provides significant stabilization to the +3 oxidation state. This could explain the stability of the iron(III) site (and lack of redox activity) in Fe−NHase. Interestingly, both $[Fe^{III}(PyPepS)_2]^-$ and $[Co^{III}(PyPepS)_2]^-$ can readily be converted to the corresponding sulfinato species by reaction with H_2O_2 or O_2, and the sulfinato species $[Fe^{III}(PyPepSO_2)_2]^-$ (structure v) exhibits an electronic absorption spectrum in water which is practically *identical* to the absorption spectrum of the Fe−NHase.[49,50] We have also shown that such oxidation can only take place when carboxamido nitrogens are present in the coordination sphere of the metal centers.[47] It is therefore evident that studies on model complexes such as ours (and those from others) do provide valuable insight into the intrinsic properties of the biological M(III) sites in NHases.

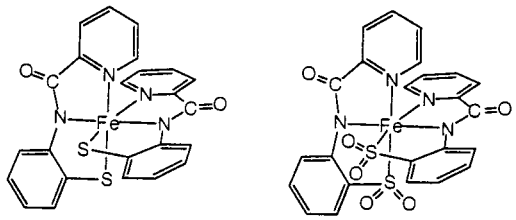

iv v

As part of our continuing effort toward elucidation of the intrinsic chemistry of the M(III) sites of the NHases, we have recently synthesized a designed pentadentate ligand *N*,*N*′-bis-(2-mercaptophenyl)pyridine-2,6-dicarboxamide ($PyPSH_4$, structure vi, H's are the dissociable carboxamide and thiol protons) that contains two carboxamide and two thiol groups. In a recent communication, we have reported the syntheses and structures of two cobalt (III) complexes of $PyPSH_4$.[51] One of these complexes, namely, $[Co^{III}(PyPS)(CN)]^{2-}$, gives rise to $[Co^{III}(PyPS)(OH)]^{2-}$ in basic solution. This cobalt(III) species with N_3S_2O coordination catalyzes a variety of nitriles under mild conditions ($T < 50$ °C, pH 9). This success prompted us to examine its coordination chemistry with iron. In this paper we report the synthesis, structure, and reactivity of the iron(III) complex with $PyPSH_4$, namely $(Et_4N)[Fe^{III}(PyPS)]$ (**1**). Complex

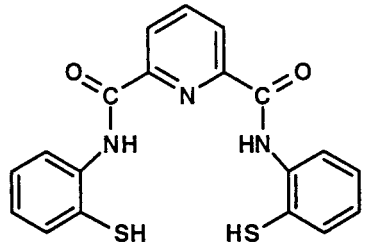

$PyPSH_4$, vi

1 contains a coordinatively unsaturated iron(III) center in a N_3S_2 coordination sphere. The iron center reversibly binds a variety of Lewis bases such as pyridine, *N*-methylimidazole, cyanide, thiolates, methanol, and water in a solvent- and temperature-dependent fashion, and such binding modulates the spin state of the iron(III) center. We report here for the first time, the pK_a of a water molecule bound to an iron(III) center with carboxamido N and thiolato S donors. We also report that complex **1** reacts with dioxygen at room temperature to afford the corresponding sulfinato species which exists as S-bonded and O-bonded forms. The structure of the O-bonded sulfinato complex $(Et_4N)[Fe^{III}(PyP\{S\underline{O}_2\}_2]^-$(**2**) is reported in this paper. In addition, we have included the synthesis and structure of the iron(II) complex $(Et_4N)_2[Fe^{II}(PyPS)]$ (**3**). And finally, the spectroscopic properties of the various iron complexes have been compared with those of the iron site in Fe−NHase to assess the success of this modeling work.

Experimental Section

Preparation of Compounds. 2,6-Pyridinedicarbonyl dichloride, 2-aminothiophenol, sodium hydride, triethylamine, triphenylmethanol, triethylsilane, tetraethylammonium cyanide, and trifluoroacetic acid were procured from Aldrich Chemical Co. and used without further purification. Small amounts (5 mL) of 98% hydrogen peroxide were prepared from 30% aqueous solution of H_2O_2 (Fisher Scientific) by following the standard procedure.[52] All of the solvents were purified by standard procedures. Standard Schlenk techniques were used during

(45) Heinrich, L.; Li, Y.; Vaussermann, J.; Chottard, G.; Chottard, J. C. *Angew. Chem., Int. Ed.* **1999**, *38*, 3526.
(46) Artaud, I.; Chatel, S.; Chauvin, A. S.; Bonnet, D.; Kopf, M. A.; Leduc, P. *Coord. Chem. Rev.* **1999**, *190−192*, 577.
(47) Noveron, J. C.; Herradora, R.; Olmstead, M. M.; Mascharak, P. K. *Inorg. Chim. Acta* **1999**, *285*, 269.
(48) Noveron, J. C.; Olmstead, M. M.; Mascharak, P. K. *Inorg. Chem.* **1998**, *37*, 1138.
(49) Tyler, L. A.; Noveron, J. C.; Olmstead, M. M.; Mascharak, P. K. *Inorg. Chem.* **1999**, *38*, 616.
(50) Tyler, L. A.; Noveron, J. C.; Olmstead, M. M.; Mascharak, P. K. *Inorg. Chem.* **2000**, *39*, 357.
(51) Noveron, J. C.; Olmstead, M. M.; Mascharak, P. K. *J. Am. Chem. Soc.* **1999**, *121*, 3553.

all syntheses to avoid exposure to dioxygen. Elemental analyses were performed by Atlantic Microlab Inc.

Trytilated Aminothiophenol. To a solution of triphenylmethanol (15.0 g, 57.6 mmol) in 100 mL of trifluoroacetic acid (TFA) was added a solution of 2-aminothiophenol (7.21 g, 57.6 mmol) in 10 mL of methylene chloride. The reaction was stirred for 1 h, and then the TFA was removed by vacuum distillation. Next, the dry residue was added to a saturated solution of aqueous $NaHCO_3$ and allowed to stir for 1 h. The mixture was then extracted with 150 mL of chloroform, and the organic layer was collected and dried with anhydrous $MgSO_4$. The solution was filtrated, and the chloroform was removed by vacuum distillation. The solid residue thus obtained was recrystallized from methanol and dried under vacuum for 24 h. Yield: 16.5 g (78%). ^{1}H NMR spectrum ($CDCl_3$, 250 MHz) δ from TMS: 3.63 (s, NH_2), 6.46 (dd, 2H), 7.04 (t, 2H), 7.37 (dd, 6H, Try CH's), 7.25 (m, 9H, Try CH's). ^{13}C NMR spectrum ($CDCl_3$, 62.5 MHz) δ 70.8, 105.2, 115.0, 116.2, 117.9, 126.6, 127.5, 129.9, 137.8, 144.3, 151.3. Selected IR bands (KBr pellet, cm^{-1}) 3462 (m), 3368 (m), 3053 (m), 1606 (s), 1477 (s), 1444 (s), 1310 (m), 743 (s), 701 (s).

PyPS-Try. A solution of trytilated aminothiophenol (7.21 g, 19.6 mmol) and triethylamine (3.47 g, 34.3 mmol) in 40 mL of chloroform was added dropwise to a solution of 2,6-pyridinedicarbonyl dichloride (2.0 g, 9.81 mmol) and triethylamine (3.47 g, 34.3 mmol) in 40 mL of chloroform. The mixture was allowed to react for 2 days at room temperature during which a portion of PyPS-Try (protected ligand vi) precipitated out of solution. The mixture was concentrated to 15 mL, and the precipitate was vacuum filtrated and washed with cold methanol. Yield: 6.02 g (71%). ^{1}H NMR spectrum ($CDCl_3$, 250 MHz) δ from TMS: 6.93 (t, 6H), 6.75 (t, 12H), 7.09 (d, 12H), 7.52 (dd, 4H), 8.03 (t, 1H) 8.21 (d, 2H), 8.67 (d, 2H), 10.66 (s, 2H, amide NH). ^{13}C NMR spectrum ($CDCl_3$, 62.5 MHz) δ 71.8, 119.7, 121.5, 123.8, 124.7, 126.8, 127.3, 129.5, 131.4, 138.3, 142.4, 143.2, 148.8, 161.0, 179.9. Selected IR bands (KBr pellet, cm^{-1}) 3300 (m, NH), 3015 (m), 1683 (vs, ν_{CO}), 1575 (vs), 1438 (s), 753 (s), 700 (s).

$PyPSH_4$ (vi). A batch of triethylsilane (2.68 g, 23.1 mmol) was added to a solution of PyPS-Try (5 g, 5.77 mmol) in 13 mL of TFA and 6 mL of dichloromethane, and the mixture was stirred for 15 min. The reaction mixture was then concentrated to half the original volume, and the resulting precipitate was filtered. Following removal of TFA and other volatiles in vacuo, the residue was washed three times with diethyl ether and collected by filtration. Yield: 2.05 g (94%). ^{1}H NMR spectrum ($CDCl_3$, 250 MHz) δ from TMS: 3.39 (s, 2H, SH), 7.12 (t, 2H), 7.36 (t, 2H), 7.56 (d, 2H), 8.19 (t, 1H) 8.36 (d, 2H), 8.53 (d, 2H), 10.49 (s, 2H, amide NH). ^{13}C NMR spectrum ($CDCl_3$, 62.5 MHz) δ 118.9, 122.0, 125.2, 125.8, 129.0, 134.6, 137.7, 139.7, 148.9, 161.2. Selected IR bands (KBr pellet, cm^{-1}) 3300 (m, NH), 2525 (w, SH), 1684 (vs, ν_{CO}), 1580 (vs), 1522 (s), 1445 (m), 1311 (m), 749 (m).

$(Et_4N)[Fe^{III}(PyPS)]$ (1). A batch of 0.101 g (4.22 mmol) of NaH was slowly added to a cold (4 °C) solution of $PyPSH_4$ (0.400 g, 1.05 mmol) in 15 mL of degassed DMF, and the mixture was stirred for 15 min. Next, the light orange solution was chilled to −40 °C, and a solution of $(Et_4N)[FeCl_4]$ (0.345 g, 1.05 mmol) in 5 mL of DMF was slowly added to it. The mixture was allowed to stir for 1 h at room temperature during which a blue-green color developed. The reaction mixture was concentrated to ~10 mL, and a batch of 10 mL of degassed acetonitrile was added. Slow diffusion of diethyl ether to this solution afforded large blocks of **1** after 48 h. The crystalline product was washed with methanol and vacuum-dried. Yield: 0.265 g (45%). Anal. Calcd for $C_{27}H_{31}N_4S_2O_2Fe$: C, 57.55; H, 5.54; N, 9.94. Found: C, 57.35; H, 5.61; N, 9.93. Selected IR bands (KBr pellet, cm^{-1}) 2982 (m), 1632 (vs, ν_{CO}), 1617 (vs), 1589 (vs), 1568 (m), 1449 (s), 1351 (m), 1270 (m), 1140 (m), 1061 (m), 1026 (m), 964 (m), 774 (s), 746 (s). Absorption spectrum in DMF (λ_{max}, nm (ϵ M^{-1} cm^{-1})) 650 (3700), 540 (3600), 420 (4400), 320 (11 000).

$(Et_4N)[Fe^{III}(PyP\{SO_2\}_2)]$ (2). A slurry of **1** (0.400 g, 1.05 mmol) in 40 mL of anhydrous acetone was placed in a stoppered flask of 100 mL volume, and 4 cm^3 of pure dioxygen was introduced into the flask. The mixture was stirred for 3 days at room temperature during which a red-brown color developed. The solution was then filtered, and the filtrate was concentrated to ~10 mL. Diffusion of diethyl ether to this solution afforded large red crystals after 48 h. Yield: 0.265 g (42%). Anal. Calcd for $C_{27}H_{31}N_4S_2O_6Fe$: C, 51.68; H, 4.98; N, 8.93. Found: C, 51.85; H, 4.68; N, 8.60. Selected IR bands (KBr pellet, cm^{-1}) 2966 (m), 1618 (vs, ν_{CO}), 1558 (vs), 1568 (vs), 1366 (m), 1263 (m), 1158 (m), 1070 (s, ν_{SO2}), 1026 (m), 804 (s). Absorption spectrum in DMF (λ_{max}, nm (ϵ M^{-1} cm^{-1})) 480 (3400), 360 (5500) nm.

$(Et_4N)_2[Fe^{II}(PyPS)]$ (3). A batch of 0.101 g (4.22 mmol) of NaH was added to a cold (4 °C) solution of $PyPSH_4$ (0.400 g, 1.05 mmol) in 15 mL of degassed DMF, and the mixture was stirred for 15 min. A solution of $(NEt_4)_2[FeCl_4]$ (0.345 g, 1.05 mmol) in 5 mL of DMF was then added to it dropwise, and the mixture was stirred for 1 h at room temperature during which a brown color developed. The reaction mixture was concentrated to ~5 mL, and 10 mL of degassed acetonitrile was added to it. Diffusion of diethyl ether to the resulting solution afforded large blocks of **3** after 48 h. Yield: 0.265 g (65%). Anal. Calcd for $C_{35}H_{51}N_5S_2O_2Fe$: C, 60.59; H, 7.41; N, 10.09. Found: C, 60.85; H, 7.70; N, 10.15. Selected IR bands (KBr pellet, cm^{-1}) 2976 (m), 1603 (m) 1572 (vs, ν_{CO}), 1558 (vs), 1450 (s), 1364 (m), 1260 (m), 1172 (m), 1056 (m), 1028 (m), 1000 (m), 772 (s), 757 (s). Absorption spectrum in DMF (λ_{max}, nm (ϵ M^{-1} cm^{-1})) 680 (sh), 330 (6800).

$Na_2[Fe^{III}(PyP\{SO_2\}_2)(CN)]$ (4). A solution of 55 mg (0.35 mmol) of $(Et_4N)(CN)$ in 1 mL of acetonitrile was slowly added to a slurry of 200 mg (0.35 mmol) of $(Et_4N)[Fe^{III}(PyPS)]$ in 10 mL of acetonitrile. The reaction mixture turned homogeneous almost immediately. It was then cooled to −40 °C in a slush bath, and a batch of 150 μL (6.0 mmol) of freshly prepared 98% H_2O_2 was added. The bright green mixture was stirred for 30 min at −40 °C. Addition of a solution of 108 mg (0.80 mmol) of $NaClO_4$ in 1 mL of acetonitrile to this reaction mixture afforded a green precipitate. It was filtered, washed three times with acetonitrile, and dried under vacuo. Yield: 150 mg (75%). Anal. Calcd for $C_{20}H_{11}N_4S_2O_6Na_2Fe$: C, 42.19; H, 1.95; N, 9.84. Found: C, 42.30; H, 1.81; N, 9.60. Selected IR bands (KBr pellet, cm^{-1}) 2208 (m, ν_{CN}), 1626 (vs, ν_{CO}), 1460, 1438, 1363, 1219, 1186 (s, ν_{SO2}), 1137, 762, 617. Absorption spectrum in DMF (λ_{max}, nm (ϵ M^{-1} cm^{-1})) 640 (1350), 470 (sh, 1600).

$(Et_4N)_2[Fe^{III}(PyP\{SO_2\}_2)(CN)]$ (5). To a solution of 80 mg (0.14 mmol) of $(Et_4N)[Fe^{III}(PyP\{SO_2\}_2)]$ in 40 mL of acetone was added with stirring a solution of $(Et_4N)(CN)$ (22 mg, 0.14 mmol) in 1 mL of acetonitrile. The color of the initial red solution turned green. A green precipitate formed within 10 min. The solid was filtered, washed twice with acetone, and dried in vacuo. Yield: 36 mg (40%). Anal. Calcd for $C_{36}H_{51}N_6S_2O_6Fe$: C, 55.17; H, 6.56; N, 10.72. Found: C, 54.95; H, 6.42; N, 10.91. Selected IR bands (KBr pellet, cm^{-1}) 2117 (m, ν_{CN}), 1604 (vs, ν_{CO}), 1460, 1456, 1356, 1262, 1030 (s, ν_{SO2}), 799. Absorption spectrum in DMF (λ_{max}, nm (ϵ M^{-1} cm^{-1})) 660 (1300), 425 (sh, 1800).

Studies on Binding of Donors at the Sixth Site of Iron in 1. (a) Water. Binding studies were performed with freshly prepared solutions of **1** in degassed acetone:water (30:70) mixture. Changes in the electronic absorption spectrum due to binding of water at low temperatures were monitored with the aid of a custom-designed low-temperature optical Dewar filled with the appropriate cooling bath. Approximately two minutes were necessary for the temperature to equilibrate in each case. An OMEGA temperature probe was used to monitor the temperature. The spectra were recorded with a diode-array Polytec PI UV−vis instrument. The pH of the solution mixtures was measured with a Beckman 200 pH meter. In a typical experiment, an aliquot (50 μL) of a 0.18 M solution of **1** in DMF was added to a Tris-buffer solution (2 mM) in acetone:water (30:70) mixture with its pH previously determined at 25 °C and −30 °C. The solution was then placed in a 10 mm quartz cell that fits on the custom-designed Dewar apparatus, and the absorption spectrum was recorded until the sample temperature reached −30 °C (temperature at which no further change in the spectrum was observed). Since the samples started freezing around −35 °C, the spectra were obtained at −30 °C. The spectra of the water adduct $[Fe^{III}(PyPS)(H_2O)]^-$ at different pH values were used to determine the pK_a of the water bound to the iron(III) center. That the buffer components do not coordinate to the iron(III) center of **1** in these experiments is evident from the fact that the electronic absorption

(52) Brauer, G. *Handbook of Preparative Inorganic Chemistry*; Academic Press: New York, 1963; pp 140−142.

spectrum of **1** in pure water is identical to that in 2 mM tris buffer at all temperatures. To correct for changes in absorbance values due to deposition of water vapor on the cold window and uncertainties in attaining the right pH in buffers containing 30% acetone, three measurements were performed at each pH, and the average values were used to plot the pH versus absorbance curve and calculate the pK_a of the bound water molecule in $[Fe^{III}(PyPS)(H_2O)]^-$.

(b) Methanol. An aliquot (50 μL) of a 0.18 M solution of **1** in DMF was added to 2 mL of methanol at room temperature. The solution was then placed in the 10 mm quartz cell that fits on the custom-designed Dewar apparatus, and the electronic spectrum was recorded when no further change in the spectrum was observed. Binding of methanol was complete at −60 °C.

(c) Pyridine. At room temperature, an aliquot (50 μL) of a 0.18 M solution of **1** in DMF was added to a mixture of 0.4 mL of acetone and 0.6 mL of pyridine. This mixture was then placed in the low-temperature cell. The electronic spectrum was recorded when no further change in the spectrum was observed. For pyridine, complete binding to **1** occurred at −70 °C.

(d) *N*-Methylimidazole. At room temperature, an aliquot (50 μL) of a 0.18 M solution of **1** in DMF was added to a mixture of 1 mL of acetone and 70 μL of *N*-methylimidazole. This mixture was then placed in the low-temperature cell. The electronic spectrum was recorded when no further change in the spectrum was observed (−70 °C).

(e) PhS^-. At room temperature, an aliquot (50 μL) of a 0.18 M solution of **1** in DMF was added to a mixture of 1 mL of acetone and 20 equiv of $(Et_4N)(SPh)$. This mixture was then placed in the low-temperature cell. The electronic spectrum was recorded when no further change in the spectrum was observed (−70 °C).

(f) Cyanide (CN^-). At room temperature, an aliquot (50 μL) of a 0.18 M solution of **1** in DMF was diluted in 2 mL of thoroughly degassed acetonitrile, and to it was added 1 equiv of $(Et_4N)(CN)$. The absorption spectrum of the cyanide-adduct was recorded in the same low-temperature cell. In acetonitrile, complete binding of CN^- was noted at −10 °C.

Determination of Thermodynamic Parameters of Binding of Water and Pyridine to 1. Binding studies were performed using freshly prepared solutions of **1** in aqueous acetone or in acetone/pyridine mixture. The van't Hoff equation was employed for the determination of the thermodynamic parameter ΔH, the enthalpy of formation of the six-coordinate adducts $[Fe^{III}(PyPS)(B)]^-$ (B = H_2O or py). The equilibrium constants were determined by monitoring the changes in the electronic absortion spectra at four different temperatures. Solutions of 6.9 mM of **1** were used in combination with appropriate concentrations of water or pyridine in acetone so that 30−90% of adducts were present at the four temperatures. The distinct low-temperature values were attained by the use of appropiate low-temperature slush baths. Spectral data at 420 nm was collected to calculate ΔH since it displayed the largest change in absorbance. The extinction coefficient of **1** at 420 nm was calculated at 22 °C (4400 M^{-1} cm^{-1}), −20 °C (4800 M^{-1} cm^{-1}), −40 °C (5000 M^{-1} cm^{-1}), and −75 °C (5150 M^{-1} cm^{-1}). These values were used to determine the concentration of **1** in the samples for these experiments. The equilibrium constants were calculated using eqs 1 and 2. The ΔH values for water and pyridine are −25.9 and −21.3 kcal mol^{-1}, respectively.

$$\{(Et_4N)[Fe^{III}(PyPS)(B)]\} = [\mathbf{1}\cdot B] = \frac{A - \epsilon_1[\mathbf{1}]_o}{\epsilon_{\mathbf{1}\cdot B} - \epsilon_{\mathbf{1}}} \quad (1)$$

$$K_{eq} = \frac{\{[\mathbf{1}\cdot B]\}}{\{[\mathbf{1}]_o - [\mathbf{1}\cdot B]\}\{[B]_o - [\mathbf{1}\cdot B]\}} \quad (2)$$

X-ray Data Collection and Structure Solution and Refinement. Dark green blocks of **1** were obtained by slow diffusion of diethyl ether into a DMF:acetonitrile (50:50 v/v) solution of **1**. Slow evaporation of an acetone solution of **2** afforded red needles which were suitable for diffraction studies. Brown needles of **3** were grown by slow diffusion of diethyl ether into an acetonitrile solution of the complex. Diffraction data for **1** were collected on a Siemens R3m/V machine (at 140 K), while data for complexes **2** and **3** were collected on a Bruker SMART 1000 system (at 90 K). Mo Kα radiation (λ = 0.71073 Å) was used for diffraction, and the data were solved by direct methods (SHELXS-97, Sheldrick, 1990). Only random fluctuations of <1% in the intensities of two standard reflections were observed during data collection for all the three complexes. Hydrogen atoms bonded to carbon were added geometrically and refined with the use of a riding model.

Table 1. Summary of Crystal Data and Intensity Collection and Structure Refinement Parameters for $(Et_4N)[Fe^{III}(PyPS)]$ (**1**), $(Et_4N)[Fe^{III}(PyP\{SO_2\}_2)]$ (**2**), and $(Et_4N)_2[Fe^{II}(PyPS)]$ (**3**)

	complex **1**	complex **2**	complex **3**
formula	$C_{27}H_{31}FeN_4O_2S_2$	$C_{27}H_{31}FeN_4O_6S_2$	$C_{35}H_{51}FeN_5O_2S_2$
(mol wt)	563.53	627.53	693.78
cryst color, habit	dark green block	red needle	brown needle
T, K	140 (2)	90 (2)	90 (2)
cryst system	monoclinic	monoclinic	monoclinic
space group	$P2_1/c$	$P2_1/n$	$P2_1/n$
a, Å	14.910 (5)	7.7471 (4)	9.5604 (5)
b, Å	18.369 (4)	21.4308 (12)	15.5545 (8)
c, Å	19.222 (4)	17.0590 (9)	23.6924 (13)
α, deg	90	90	90
β, deg	91.12 (2)	92.9000 (10)	90.6610 (10)
γ, deg	90	90	90
V, Å^3	5264 (2)	2828.6 (3)	3523.0 (3)
Z	8	4	4
d_{calcd}, g cm^{-3}	1.422	1.474	1.308
abs coeff, μ, mm^{-1}	0.764	0.729	0.585
GOF[a] on F^2	1.009	0.872	0.885
R1,[b] %	5.27	4.15	5.41
wR2,[c] %	9.83	9.10	11.77

[a] GOF = $\{\sum[w(F_o^2 - F_c^2)^2]/(M\text{-}N)\}^{1/2}$ (M = no. of reflections, N = no. of parameters refined). [b] R1 = $\sum||F_o| - |F_c||/\sum|F_o|$. [c] wR2 = $\{\sum[w(F_o^2 - F_c^2)^2]/\sum[w(F_o^2)^2]\}^{1/2}$.

Machine parameters, crystal data, and data collection parameters are summerized in Table 1. Selected bond distances and angles are listed in Table 2. The rest of the crystallographic data has been submitted as Supporting Information.

Other Physical Measurements. The electronic absorption spectra were measured on a Perkin-Elmer Lambda 9 spectrophotometer. A Perkin-Elmer 1600 FTIR spectrophotometer was used to monitor the infrared (IR) spectra. ^1H and ^{13}C NMR spectra were recorded on a Bruker 250 machine. EPR spectra were monitored at X-band frequencies by using a Bruker ESP-300 spectrometer. Room-temperature magnetic measurements on solid samples were made with a Johnson-Matthey magnetic susceptibility balance. Electrochemical measurements were performed with standard Princeton Applied Research instrumentation and a Pt inlay electrode. Potentials were measured at 25 °C versus an aqueous saturated calomel electrode (SCE) as reference. The pK_a of the bound water in $[Fe^{III}(PyPS)(H_2O)]^-$ was determined by fitting the plot of pH versus absorbance at 420 nm with the aid of MATLAB package (see Supporting Information) and by using the function $A = f_{HA}\,a_{HA} + f_{B-}\,a_{B-}$ where A is total absorbance, a_{HA} and a_{B-} are the absorbances of the protonated and deprotonated species at 420 nm respectively, and

$$f_{HA} = \frac{1}{\frac{K_a}{[H^+]} + 1}, \quad f_{B-} = \frac{1}{\frac{[H^+]}{K_a} + 1}$$

Results and Discussion

Syntheses of the Complexes. In a series of papers published from our laboratory, we have described the syntheses and structures of iron(III) (and iron(II)) and cobalt(III) complexes that contain carboxamido N coordination along with other donor sets.[53,54,58−63] The discovery of the highly unprecedented coordination sphere at the iron and cobalt centers in NHases has prompted us to further explore the coordination chemistry of these two metals with new ligands with carboxamide and thiolate groups.[48−51] In the present study, we have utilized the designed ligand $PyPSH_4$ which comprises two carboxamide and two

Table 2. Selected Bond Distances (Å) and Angles (deg) for **1**−**3**

$(Et_4N)[Fe^{III}(PyPS)]$ (**1**)					
Bond Distances					
Fe(1)−N(1)	2.035 (3)	S(1)−C(1)	1.770 (4)	N(1)−C(7)	1.355 (5)
Fe(1)−N(2)	2.099 (3)	S(2)−C(19)	1.773 (4)	N(2)−C(8)	1.324 (5)
Fe(1)−N(3)	2.041 (3)	O(1)−C(7)	1.237 (5)	N(3)−C(13)	1.354 (5)
Fe(1)−S(1)	2.3147 (13)	O(2)−C(13)	1.242 (5)	N(3)−C(14)	1.408 (5)
Fe(1)−S(2)	2.3104 (13)	N(1)−C(6)	1.423 (5)	C(17)−C(18)	1.383 (7)
Bond Angles					
N(1)−Fe(1)−N(3)	150.28 (14)	N(2)−Fe(1)−S(2)	126.21 (10)		
N(3)−Fe(1)−N(2)	75.01 (14)	S(2)−Fe(1)−S(1)	109.53 (5)		
N(3)−Fe(1)−S(2)	83.95 (10)	C(2)−C(1)−S(1)	120.7 (3)		
N(1)−Fe(1)−S(1)	84.17 (10)	C(1)−C(6)−N(1)	115.2 (4)		
N(1)−Fe(1)−N(2)	75.28 (14)	O(1)−C(7)−C(8)	120.2 (4)		
N(1)−Fe(1)−S(2)	114.33 (11)	C(15)−C(14)−N(3)	124.0 (4)		
$(Et_4N)[Fe^{III}(PyP\{SO_2\}_2)]$ (**2**)					
Bond Distances					
Fe−O(1)	1.9112 (14)	S(1)−O(1)	1.5633 (16)	O(3)−C(7)	1.229 (2)
Fe−O(6)	1.9127 (15)	S(1)−O(2)	1.4788 (16)	O(4)−C(13)	1.223 (3)
Fe−N(1)	2.0201 (17)	S(1)−C(1)	1.798 (2)	N(3)−C(13)	1.360 (3)
Fe−N(2)	2.0708 (17)	S(2)−O(5A)	1.431 (2)	N(1)−C(7)	1.364 (2)
Fe−N(3)	2.0175 (17)	S(2)−C(19)	1.809 (2)	C(12)−C(13)	1.514 (3)
Bond Angles					
O(1)−Fe−O(6)	106.24 (7)	O(5A)−S(2)−O(6)	107.68 (11)		
O(1)−Fe−N(1)	94.81 (6)	O(2)−S(1)−O(1)	108.85 (9)		
O(1)−Fe−N(3)	101.89 (6)	O(2)−S(1)−C(1)	104.73 (9)		
O(6)−Fe−N(3)	93.13 (7)	O(1)−S(1)−C(1)	103.12 (9)		
O(6)−Fe−N(2)	125.75 (7)	S(2)−O(6)−Fe	124.31 (9)		
O(6)−Fe−N(1)	104.33 (7)	C(6)−N(1)−Fe	118.43 (12)		
O(1)−Fe−N(2)	127.96 (7)	C(8)−N(2)−Fe	118.43 (14)		
N(3)−Fe−N(1)	151.43 (7)	O(4)−C(13)−C(12)	121.30 (19)		
N(3)−Fe−N(2)	75.42 (7)	C(15)−C(16)−C(17)	120.6 (2)		
$(Et_4N)_2[Fe^{II}(PyPS)]$ (**3**)					
Bond Distances					
Fe−N(1)	2.160(2)	S(1)−C(1)	1.778(3)	N(1)−C(7)	1.326(4)
Fe−N(2)	2.129(2)	S(2)−C(19)	1.768(3)	N(2)−C(8)	1.332(4)
Fe−N(3)	2.179(2)	O(1)−C(7)	1.249(3)	N(3)−C(13)	1.344(4)
Fe−S(1)	2.4094(8)	O(2)−C(13)	1.242(3)	N(3)−C(14)	1.389(4)
Fe−S(2)	2.3783(8)	N(1)−C(6)	1.407(4)	C(17)−C(18)	1.373(5)
Bond Angles					
N(2)−Fe−N(1)	73.07(9)	N(1)−Fe−S(2)	120.79(7)	C(2)−C(1)−S(1)	120.2(3)
N(2)−Fe−N(3)	73.33(9)	N(3)−Fe−S(2)	79.85(7)	N(1)−C(6)−C(1)	116.0(3)
N(1)−Fe−N(3)	146.34(10)	N(1)−Fe−S(1)	80.00(8)	O(1)−C(7)−C(8)	118.1(3)
N(2)−Fe−S(2)	128.44(77)	S(2)−Fe−S(1)	101.05(3)	N(3)−C(14)−C(15)	125.9(3)

thiolate groups. The fully deprotonated $PyPS^{4-}$ ligand binds iron(III) in DMF at low temperature to form $[Fe^{III}(PyPS)]^-$ without any complication arising out of reduction of the iron center and formation of disulfide.[48,56,57] This behavior is in contrast to the reaction of iron(III) with the corresponding Schiff base ligand 2,6-bis[1-methyl-2-(2-thiolophenyl)-2-azaethene]-pyridine[55] which only gives rise to the iron(II) complex. It is evident that coordination of the carboxamido nitrogens provides stability to iron(III) centers and prohibits reduction in case of $PyPS.^{4-}$ This is further supported by the fact that when one uses only 2 equiv of NaH, reaction of $PyPSH_2^{2-}$ (only the thiolate groups are deprotonated) with iron(III) leads to autoredox reaction resulting in the formation of polymeric products of iron(II) and disulfides.[62,63] The fully deprotonated $PyPS^{4-}$, however, affords the iron(II) complex $[Fe^{II}(PyPS)]^{2-}$ when one starts with an iron(II) source.

Solutions of **1** and **3** are sensitive to dioxygen. However, when a solution of **1** is stirred with controlled amount (∼12 equiv) of dioxygen in dry acetone, **1** is smoothly converted into the sulfinato species **2** in which both thiolato groups are converted into sulfinato groups. To date, we have only been able to isolate the O-bonded isomer of **2**. In absence of H-bonding interactions that involve the sulfinic O atoms (like in the enzyme), the oxophilic nature of the iron(III) center and strain in the five-membered chelate rings of **1** both prefer formation of the O-bonded isomer upon oxidation. It is quite possible that the

(53) Brown, S. J.; Olmstead, M. M.; Mascharak, P. K. *Inorg. Chem.* **1990**, *29*, 3229.
(54) Tan, J. D.; Hudson, S. E.; Brown, S. J.; Olmstead, M. M.; Mascharak, P. K. *J. Am. Chem. Soc.* **1992**, *114*, 3841.
(55) Chavez, F. A.; Rowland, J. M.; Olmstead, M. M.; Mascharak, P. K. *J. Am. Chem. Soc.* **1998**, *120*, 9015.
(56) Chavez, F. A.; Olmstead, M. M.; Mascharak, P. K. *Inorg. Chem.* **1997**, *36*, 6323.
(57) Chavez, F. A.; Olmstead, M. M.; Mascharak, P. K. *Inorg. Chem.* **1996**, *35*, 1410.
(58) Marlin, D. S.; Olmstead, M. M.; Mascharak, P. K. *Inorg. Chem.* **1999**, *38*, 3258.
(59) Marlin, D. S.; Olmstead, M. M.; Mascharak, P. K. *Inorg. Chim. Acta* **2000**, *297*, 106.
(60) Marlin, D. S.; Mascharak, P. K. *Chem. Soc. Rev.* **2000**, *29*, 69.
(61) Lindoy, L. F.; Busch, D. H. *Inorg. Chem.* **1974**, *13*, 2494.
(62) Holm, R. H.; Ibers, J. A. In *Iron-Sulfur Proteins*; Lovenberg, W., Ed.; Academic Press: New York, 1997; Vol. III, Chapter 7.
(63) Ellis, K. J.; Lappin, A. G.; McAuley, A. *J. Chem. Soc., Dalton Trans.* **1975**, 1931.

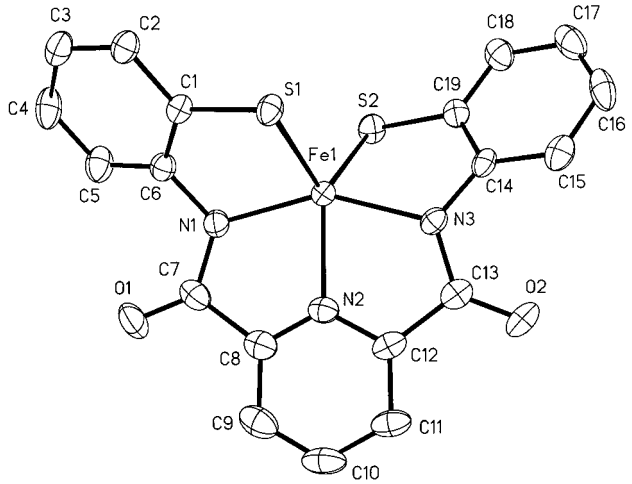

Figure 2. Thermal ellipsoid plot (probability level 50%) of $[Fe^{III}(PyPS)]^-$, the anion of complex **1**. H atoms are omitted for the sake of clarity.

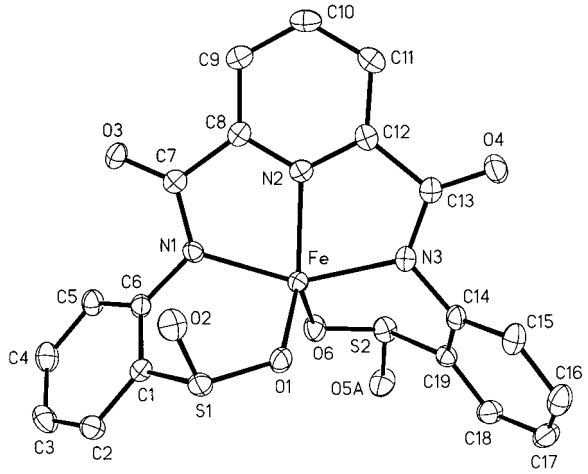

Figure 3. Thermal ellipsoid plot (probability level 50%) of $[Fe^{III}(PyP\{SO_2\}_2)]^-$, the anion of complex **2**. H atoms are omitted for the sake of clarity.

O-bonded isomer of **2** is more stable than the S-bonded one. Further support for this statement comes from the successful isolation of the O-bonded sulfinato species $(Et_4N)_2[Fe^{III}(L\text{-}O_2)]$ (structure ii) by Chottard and co-workers.[45]

Structure of $(Et_4N)[Fe^{III}(PyPS)]$ (1). The structure of **1** consists of discrete cations and monomeric anions (shown in Figure 2) and is devoid of any solvent molecules of crystallization. The tetraanionic pentadentate ligand $PyPS^{4-}$ is coordinated to the iron(III) center in a distorted trigonal bipyramidal fashion to give rise to a N_3S_2 coordination sphere. There is no interaction between the iron(III) centers (minimum Fe−Fe distance = 8 Å, Figure S1, Supporting Information). This is in contrast to the structure of the cobalt(III) complex of $PyPS^{4-}$ which is dimeric.[51] In the dimeric $[Co_2(PyPS)_2]^{2-}$ anion, the sixth site of each cobalt is ligated to one of the bound thiolato sulfurs of the other $[Co^{III}(PyPS)]^-$ moiety. The propensity of the low-spin Co(III) complexes for octahedral coordination is most possibly responsible for this difference. Close examination of the two structures also reveals that in the dimeric cobalt(III) complex, the $PyPS^{4-}$ ligand frame is wrapped around the two cobalt centers in identical helical configurations. The asymmetric unit of **1** on the other hand, contains two $[Fe^{III}(PyPS)]^-$ anions with opposite configurations pertaining to the two possible helical orientations the ligand can adopt at the iron(III) center (Figure S1). Results of solution magnetic measurements and EPR experiments at low temperatures (down to 4 K) indicate that the anions of **1** remain mononuclear at all temperatures. The reason for the different ways of ligation of the $PyPS^{4-}$ ligand frame around cobalt(III) and iron(III) remains unclear at this time.

In complex **1**, the average Fe(III)−N_{amido} distance is 2.04 Å (Table 2) and compares well with the corresponding distance reported for NHase, 2.07 Å (average value).[29] This value is somewhat longer compared to the Fe(III)−N_{amido} distances observed in other carboxamido complexes of trivalent iron[46,63,64] including Chottard's complex ii.[45] The average Fe(III)−S_{thio} (thio = thiolate) distance in **1** (2.31 Å) also compares well with the corresponding average Fe(III)−S_{thio} distance reported for NHase (2.32 Å)[29] and for other complexes with Fe(III)−S_{thio} coordination (2.25−2.30 Å).[46,48,65−67] The model complex $[Fe^{III}S_2{}^{Me2}N_3(Pr,Pr)]^+$ (structure i) from Kovacs' group however exhibits a shorter Fe(III)−S_{thio} distance (2.13 Å) presumably due to constraints in the ligand frame.[43] Presence of four sets of five-membered rings in the coordination sphere of iron in **1** gives rise to smaller bond angles such as S(1)−Fe−S(2) (109.53° instead of 120°) and N(1)−Fe−N(3) (150.28° instead of 180°). The same fact opens up both S(1)−Fe−N(2) and S(2)−Fe−N(2) angles and allows further coordination to generate six-coordinate complexes (vide infra).

Structure of $(Et_4N)[Fe^{III}(PyP\{\underline{SO_2}\}_2]$ (2). The structure of the anion of **2** (Figure 3) clearly demonstrates that the two-coordinated thiolato sulfurs are converted to sulfinato groups and the sulfinato groups are coordinated to iron through one of the oxygen atoms. The coordination geometry around iron is still distorted trigonal bipyramidal and the sulfinato groups reside in the basal plane. The binding mode of the sulfinato groups in **1** resemble that observed in Chottard's complex ii.[45] In both cases, changes from S-coordination to O-coordination occurs upon oxidation of the ligated thiolato sulfurs. It is however interesting to note that oxidation of the six-coordinated iron(III) complex $[Fe^{III}(PyPepS)_2]^-$ (structure iv) affords the S-bonded sulfinato species $[Fe^{III}(PyPep\underline{SO_2})_2]^-$ (structure v) without isomerization to the O-bonded species.[49]

Conversion of **1** into **2** does not bring any significant change in the average Fe(III)−N_{amido} distances. In complex **2**, the average Fe(III)−N_{amido} distance is 2.02 Å. The average Fe(III)−$S\underline{O_2}$ ($S\underline{O_2}$ denotes O-bonded sulfinato group) bond distance (1.91 Å) in **2** compares well with the only other known Fe(III)−$S\underline{O_2}$ distance (2.00 Å) reported for complex $[Fe^{III}(L\text{-}O_2)]^-$ (structure ii).[45] The bond angles of the sulfinate groups (like O(1)−S(1)−O(2) = 108.85°) indicates sp^3 hybridized sulfur atoms in **2**.

Structure of $(Et_4N)_2[Fe^{II}(PyPS)]$ (3). The structure of the anion of this iron(II) complex is shown in Figure 4 while selected bond distances and angles are collected in Table 2. The iron(II) center in the anion of **3** is ligated to the tetraanionic ligand $PyPS^{4-}$ in a distorted trigonal bipyramidal fashion. The N_3S_2 coordination sphere is similar to that observed in the corresponding iron(III) complex **1** except for the fact that the bond distances are somewhat longer.in case of **3**. For example, the average Fe(II)−N_{amido} and Fe(II)−S_{thio} bond distances in **3** are 2.16 and 2.38 Å respectively. Overall, the Fe(II)−N_{amido}

(64) Ray, M.; Ghosh, D.; Shirin, Z.; Mukherjee, R. *Inorg. Chem.* **1997**, *36*, 3568.
(65) Hsu, H.; Koch, S. A.; Popescu, C. V.; Munk, E. *J. Am. Chem. Soc.* **1997**, *119*, 8371.
(66) Millar, M.; Lee, J. F.; Koch, S. A.; Fikar, R. *Inorg. Chem.* **1982**, *21*, 4105.
(67) Shoner, S. C.; Barnhart, D.; Kovacs, J. A. *Inorg. Chem.* **1995**, *34*, 4517.

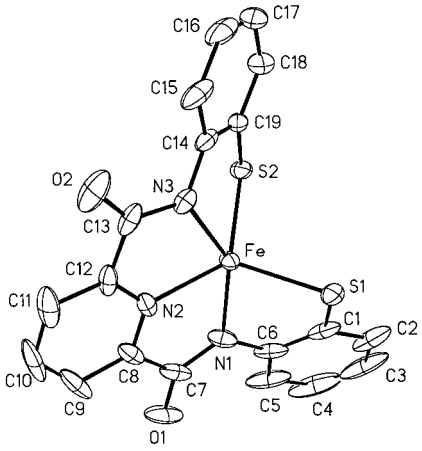

Figure 4. Thermal ellipsoid plot (probability level 50%) of $[Fe^{II}(PyPS)]^{2-}$, the anion of complex **3**. H atoms are omitted for the sake of clarity.

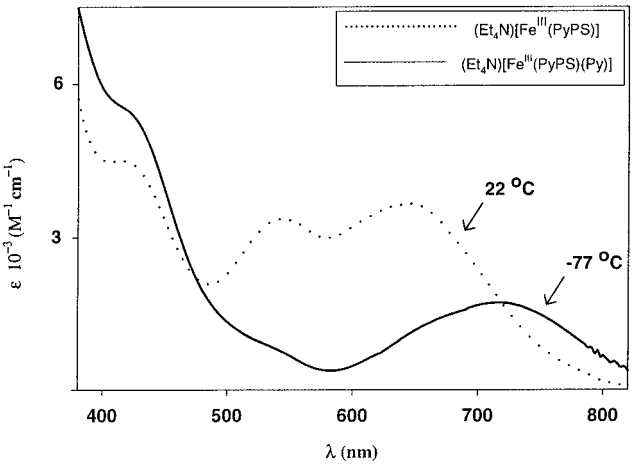

Figure 5. Electronic absorption spectra of $(Et_4N)[Fe^{III}(PyPS)]$ (complex **1**, dotted line) in DMF and $(Et_4N)[Fe^{III}(PyPS)(py)]$ (solid line) in acetone/py (2:3) mixture. The temperatures of measurements are indicated. See Experimental Section for detail.

distance of **3** is considerably longer than that noted for other iron(II) complexes with ligated carboxamido nitrogens.[53]

Properties of $(Et_4N)[Fe^{III}(PyPS)]$ (1). Coordination of the deprotonated carboxamido nitrogens to the iron(III) center of **1** is evidenced by the red-shift of the carbonyl stretching frequency (ν_{co}) from 1680 cm^{-1} in free ligand to 1632 cm^{-1} in the complex. Similar red shift has been noted for $(Et_4N)[Fe^{III}(PyPepS)_2]$[48] and other iron(III) complexes with coordinated carboxamido nitrogens.[63] The electronic absorption spectrum of **1** in solvents such as DMF and acetone consists of three strong bands with maxima at 650, 540, and 420 nm (Figure 5). These absorptions arise from thiolate-to-iron(III) charge-transfer transitions and are not present in the absorption spectrum of the iron(II) complex **3**. The overlapping bands at 650 and 540 nm are responsible for the blue-green color of **1**. Binding of ligands such as pyridine to the iron(III) center of **1** (vide infra) results in green solutions which exhibit absorption spectra much like NHase (Figure 5). It is important to note that to date, no pentacoordinate iron(III) complex with N,S coordination has afforded an absorption spectrum which resembles the absorption spectrum of NHase (broad bands at 700 and 420 nm) that gives the enzyme its characteristic green color. For instance, the pentacoordinate iron(III) complex $[Fe^{III}S_2{}^{Me2}N_3(Pr,Pr)]PF_6$ (structure i) is red and exhibits band maxima at 450 and 380 nm.[43] The other two model complexes $[Fe^{III}(L\text{-}O_2)]^-$ (structure ii) and $[Fe^{III}(N_2S_2)Cl]^{2-}$ (structure iii) are also red and exhibit absorptions at 475 (in acetonitrile) and 500 nm (in dichloromethane), respectively.[45,46] Nevertheless it is interesting to note that binding of azide (N_3^-) to $[Fe^{III}S_2{}^{Me2}N_3(Pr,Pr)]^-$ results in a green solution (absorption maxima at 708 and 460 nm). Since binding of many Lewis bases to the iron(III) center of **1** also gives rise to green solutions with absorptions around 700 nm, it appears that the iron site in the enzyme most possibly is six-coordinate.

The iron(III) center in **1** is high-spin and exhibits a magnetic moment of 6.1 μ_B in the polycrystalline state and in DMF solution at 300 K. It also exhibits a broad EPR spectrum with $g = 8.32$, 5.19, 4.14, and 2.11 at 4 K in DMF glass. The spectrum, typical of high-spin iron(III) in distorted crystal field, arises from transitions associated with all three Kramers' doublets.[68,69] The spin states of iron(III) centers in complexes with N,S coordination show wide variabilities and the reason(s) for such behavior is not clear at the present time. For example, despite strong chelation effect of the ligand frames, **1** contains a high-spin iron(III) center while Chottard's model complex $NEt_4[Fe^{III}(L\text{-}O_2)]$ exhibits intermediate spin ($S = {}^3/_2$) at all temperatures. The iron(III) center in Kovacs' pentacoordinate complex $[Fe^{III}S_2{}^{Me2}N_3(Pr,Pr)]PF_6$ is predominantly low-spin ($S = {}^1/_2$) below 50 K while the high-spin state ($S = {}^5/_2$) gets significantly populated above 150 K. The complex $[Fe^{III}(N_2S_2)Cl]^{2-}$ has intermediate spin ($S = {}^3/_2$) at low temperatures. All these complexes are pentacoordinate and contain N,S coordination spheres. Wieghardt and co-workers have reported two octahedral iron(III) complexes of macrocyclic N_3S_3 ligands which show spin equilibrium between high-spin ($S = {}^5/_2$) and low-spin ($S = {}^1/_2$) forms.[70] In contrast, a few octahedral iron(III) complexes with N, S coordination have also been reported that exist in low-spin ($S = {}^1/_2$) forms at all temperatures. These include $[Fe^{III}(ADIT)_2]^+$,[67] $[Fe(L)_2]^+$ (L = 2-aminoethylthiosalicylideneimine),[71] $[Fe^{III}(PyArS)_2]^+$,[47] $[Fe^{III}(PyRS)_2]^+$,[47] $[Fe^{III}(PypepS)_2]^-$,[48] and $[Fe^{III}(PypepSO_2)_2]^-$.[49] Collectively, these examples indicate that six-coordinate iron(III) complexes with N,S coordination are mostly low-spin. This hypothesis is further supported by the fact that both **1** and $[Fe^{III}S_2{}^{Me2}N_3(Pr,Pr)]PF_6$ afford low-spin adducts with CN^- (vide infra) and NO, respectively. Again, these results corroborate the proposition that the biological iron site is six-coordinate.[18,32]

Coordination of the carboxamido nitrogens provides stability to the +3 oxidation state of iron in **1**. This is evidenced by the reduction potential of **1**. In DMF, **1** exhibits a reversible cyclic voltammogram (Figure 6) with half wave potential ($E_{1/2}$) of −0.65 V (vs SCE). A $E_{1/2}$ value of −0.27 V (vs SCE) has been reported for $[Fe^{III}S_2N_3(Pr,Pr)]PF_6$, a complex with no carboxamido nitrogen in the coordination sphere.[43] We attribute the greater stability of the iron(III) center in **1** due to the coordinated carboxamido nitrogens. The reduction potential of the iron(III) center of the NHase from *Rhodococcus* sp. R312 in the presence of butyric acid has recently been measured.[46] The $E_{1/2}$ value (−0.48 V vs SCE) suggests that the biological iron(III) site is not easily reduced. It is quite evident that extra stability due to coordination of the carboxamido nitrogens prevents redox processes at the iron(III) site in NHase and allows it to act more like a Lewis acid. The reversibility of the voltammogram in Figure 6 first prompted us to synthesize the iron(II) complex **3**.

(68) Drago, R. In *Physical Methods for Chemists*, 2nd ed.; Saunders College Publishing: Ft. Worth, 1977; pp 583−586.
(69) Oosterhuis, W. T. *Struct. Bonding (Berlin)* **1974**, *20*, 59.
(70) Beissel, T.; Burger, K. S.; Voigt, G.; Wieghardt, K.; Butzlaff, C.; Trautwein, A. X. *Inorg. Chem.* **1993**, *32*, 124.
(71) Fallon, G. D.; Gatehouse, B. M. *J. Chem. Soc., Dalton Trans.* **1975**, 1344.

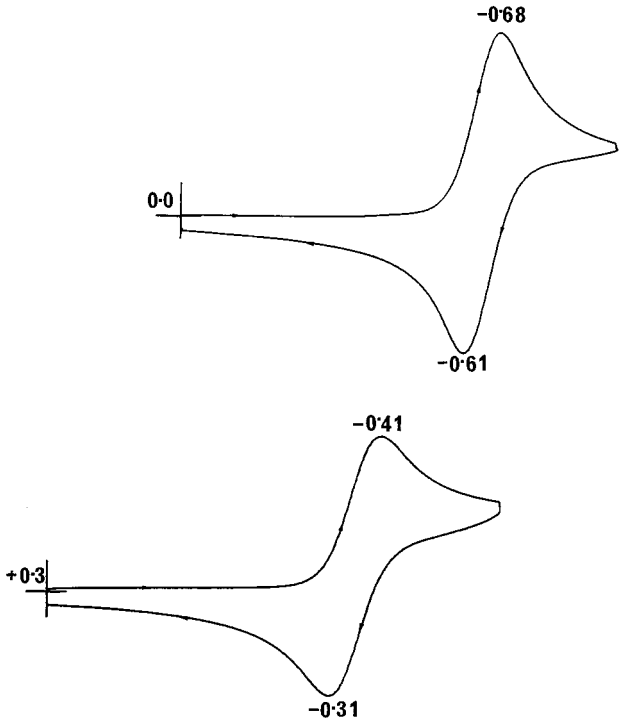

Figure 6. Cyclic voltammograms of 5mM solutions of $(Et_4N)[Fe^{III}(PyPS)]$ (**1**) (top) and $(Et_4N)[Fe^{III}(PyP\{SO_2\}_2)]$ (**2**) (bottom) in DMF (0.1 M $(Et_4N)(ClO_4)$; Pt electrode; 100 mV/s scan speed). Potentials are indicated vs aqueous SCE.

Incidentally, **3** is the first example of an iron(II) species with ligated carboxamido N and thiolato S donors.

Properties of $(Et_4N)[Fe^{III}(PyP\{SO_2\}_2)]$(2). The infrared spectrum of **2** shows a moderately strong band at 1070 cm^{-1}, corresponding to the S−O stretching (ν_{SO2}) of the O-bonded sulfinato groups. This value compares well with the ν_{SO2} (1040 cm^{-1}) noted for the model complex $NEt_4[Fe^{III}(L\text{-}O_2)]$ (structure ii).[45] Complex **2** also exhibits strong ν_{CO} stretching at 1618 cm^{-1}, a value that confirms the presence of coordinated carboxamido groups. A solution of **2** in DMF displays bands at 480 and 360 nm. Overall, this electronic absorption spectrum resembles that of the two pentacoordinate model complexes $[Fe^{III}(L\text{-}O_2)]$ (450 and 380 nm) and $[Fe^{III}(N_2S_2)Cl]$ (500 and 390 nm) with coordinated carboxamido nitrogens.[45,46]

Both the magnetic moment at 300 K (5.8 μ_B, polycrystalline sample) and the EPR spectrum ($g = 4.27$, DMF glass, 77 K) of **2** indicate that the iron(III) center exists in the high-spin state. The reduction potential of **2** in DMF (−0.36 V vs SCE, Figure 6) demonstrates that conversion of the bound thiolato groups to the O-bonded sulfinato groups reduces the stability of the iron(III) center. It will be interesting to study the effect of the posttranslational modifications of the bound Cys-residues on the overall redox potential of the iron(III) site in NHase.

Properties of $(Et_4N)_2[Fe^{II}(PyPS)]$ (3). The infrared spectrum of **3** exhibits a strong ν_{CO} stretching at 1572 cm^{-1} for the bound carboxamide groups. As discussed in our previous papers, ν_{CO} stretching frequencies of iron(II)−amides are always lower than those of the corresponding iron(III)−amides due to greater contribution of the imminolate ($^-O-C{=}N-$) tautomeric form of the bound peptide moiety.[53,63] Complexes **1** and **3** are no exception in this regard. The iron(II) center in **3** exists in high-spin state as evidenced by the magnetic moment of the complex (4.9 μ_B, polycrystalline sample) at 300 K. Upon exposure to dioxygen, **3** in DMF is readily converted into **1**. The oxidation can also be achieved by ferrocenium salts.

Reactivity of $(Et_4N)[Fe^{III}(PyPS)]$ Toward a Sixth Ligand. The trigonal bipyramidal complex **1** comprises an open angle (N(2)−Fe−S(2)) of 127.34° and is expected to bind a sixth ligand. We discovered that ligands with good Lewis base strength binds to the iron(III) center of **1** in a temperature- and solvent-dependent fashion. Ligands such as pyridine, *N*-methylimidazole, methanol, aryl thiolates, methoxide, and water all bind to **1** at low temperatures ($T < 0$ °C) to generate six-coordinate species. Binding of CN^- occurs at room temperature, and the cyanide adduct ($\nu_{CN} = 2024$ cm^{-1}, $g = 2.29$, 2.10, 1.97, Figure 7) can be isolated from acetonitrile solution in high yield. Although we do not have a structure of $(Et_4N)_2[Fe^{III}(PyPS)(CN)]$ as of yet, the corresponding cobalt(III) species has been structurally characterized.[51] The spectroscopic parameters of these six-coordinate adducts indicate a general structure (structure vii) that includes two carboxamido nitrogens coordinated in the basal plane of iron and two coordinated thiolato S donors *cis* to each other. One of the thiolato S occupies an axial position, *trans* to the incoming ligand L. These structural features are similar to those observed for the iron center in NHase (Figure 1) and hence the properties of these adducts deserve attention.

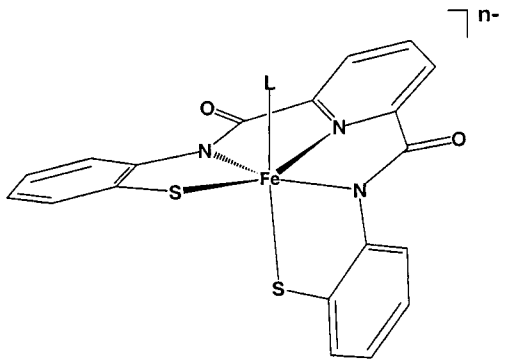

vii

In the present study, binding of ligands at the sixth site of the iron(III) center in **1** has been studied at different temperatures and in different solvents to explore the basic chemistry associated with an iron(III) center with ligated carboxamido N and thiolato S donors. To begin with, we found that binding of ligands is dependent on both the solvent and the temperature of binding. For example, when **1** is dissolved in methanol and cooled, the absorption spectrum changes slowly and finally at −60 °C, affords the methanol adduct $[Fe(PyPS)(HOMe)]^-$ which exhibits bands at 790 and 550 nm. This six-coordinate species is low-spin and displays a rhombic EPR signal with $g = 2.23$, 2.20, and 1.93. It is important to note that $[Fe(PyPS)(HOMe)]^-$ with a N,S,O coordination sphere around iron(III) exhibits spectral properties that are similar to that of the iron(III) center of NHase. Similar experiments with solutions of **1** in acetone and different ligands show that complete binding of L occurs for *N*-methylimidazole at −60 °C, for pyridine at −60 °C, and for PhS^- at −30 °C. In all cases, the six-coordinate adducts exhibit low-spin EPR spectra (Figure 7) and have one strong absorption band near 700 nm (Table 3, Figure S2, Supporting Information). Clearly, the iron(III) center in **1** with ligated carboxamido N and thiolato S donors binds to a wide variety of neutral and anionic ligands with varying affinities. It is, however, interesting to note that the iron(III) center of **1** shows *no* affinity to nitriles even at −100 °C. Kovacs and coworkers have reported that the iron(III) center in $[Fe^{III}S_2N_3(Pr,Pr)]PF_6$ binds to azide (N_3^-) and NO at low temperatures

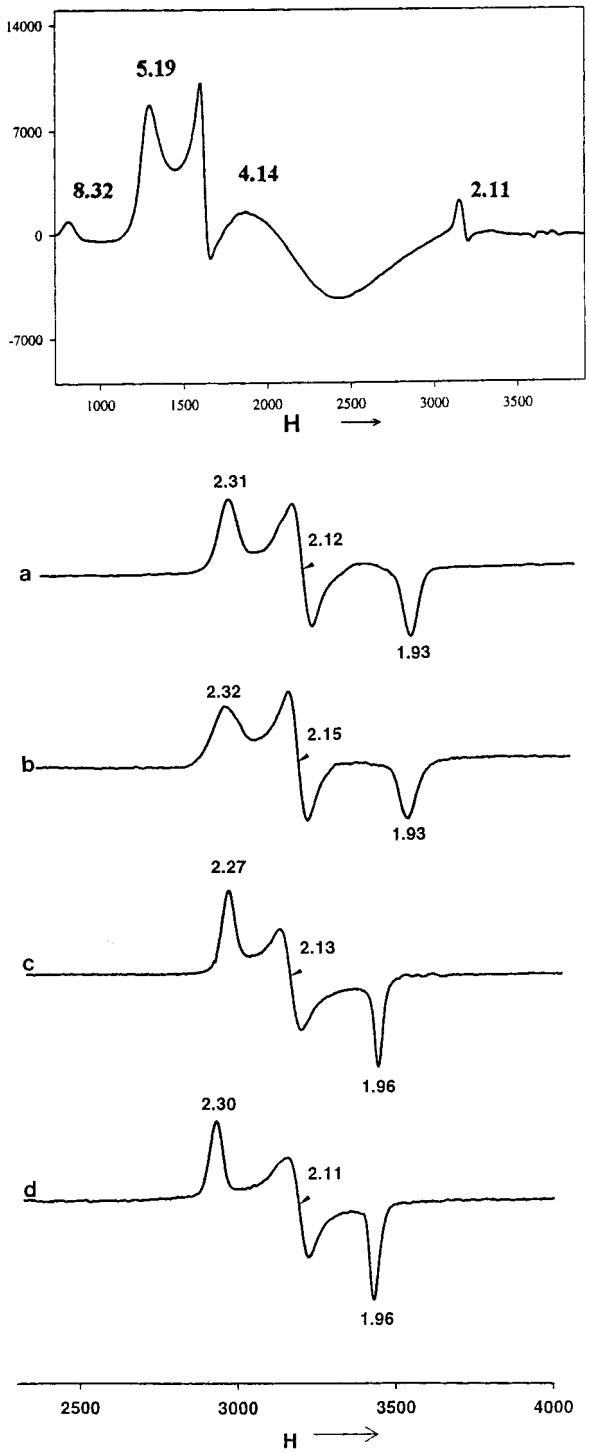

Figure 7. Top panel: X-band EPR spectrum of $[Fe(PyPS)]^-$ at 4 K. Bottom panel: X-band EPR spectra of (a) $[Fe^{III}(PyPS)(OH)]^{2-}$, (b) $[Fe^{III}(PyPS)(N\text{-}MeIm)]^-$, (c) $[Fe^{III}(PyPS)(SPh)]^{2-}$ and (d) $[Fe^{III}(PyPS)(CN)]^{2-}$ at 80 K. See experimental details for generation of these adducts. Sample concentration: 3 mM in all cases. The *g* values are tabulated in Table 3. Spectrometer settings: microwave frequency, 9.43 GHz; microwave power, 10 mW; modulation frequency, 100 kHz; modulation amplitude, 2G.

but has no affinity toward nitriles.[43] Therefore, it seems unlikely that the mechanism of catalysis by NHase involves binding of the nitrile substrates to the iron(III) center (inner-sphere mechanism).

Formation of $(Et_4N)[Fe^{III}(PyPS)(H_2O)]$ and its Reactivity. To investigate the other suggested mechanism for nitrile hydration, namely, hydration by an iron(III)-bound hydroxide (outer-sphere mechanism), we have studied the binding of water at the sixth site of iron(III) in **1** and determined the pK_a of such a bound water molecule. Early EPR[18] and ENDOR[32] data indicated that the active site of NHase contains a water molecule bound to the apical site of the iron(III) center. On the basis of the structures of other hydrolases, it has also been proposed that the bound water at the metal center is in the hydroxide form and there is one ENDOR work which supports the presence of a hydroxide group bonded to the apical site of the metal center in NHase.[34] We discovered that complex **1** binds water at low temperatures and results in the formation of $[Fe^{III}(PyPS)(H_2O)]^-$, a reaction that can be followed by monitoring changes in the absorption spectrum of **1** in an acetone:water (30:70) mixture (Figure 8). As the temperature of the solution is decreased, changes in the absorption spectrum are noticed with the appearance of two isosbestic points at 590 and 790 nm. No change is observed beyond −30 °C when the formation of $[Fe^{III}(PyPS)(H_2O)]^-$ becomes complete (acetone does not bind to the iron(III) center of **1** even at −94 °C, its freezing point).

These changes are completely reversible and as one expects, is sensitive to the pH of the solution. The plot of the absorbance of the 420 nm band of the final spectra of such solutions of **1** at −30 °C versus the pH values (Figure S3, Supporting Information) affords an apparent value of 6.3 ± 0.4 for the pK_a of the bound water molecule in $[Fe^{III}(PyPS)(H_2O)]^-$ at −30 °C. We have previously reported that the pK_a of the bound water in $[Co^{III}(PyPS)(H_2O)]^-$ at room temperature is 8.3.[51] Replacement of cobalt(III) with iron(III) in $[M^{III}(PyPS)(H_2O)]^-$ apparently increases the acidity of the bound water molecule. The pK_a of water bound to other iron(III) complexes have been reported. For example, in $[Fe^{III}(3,4\text{-}TDTA)(H_2O)]^-$ (TDTA is a tetraanionic ligand with N_2O_4 donor set), the pK_a of the bound water is 8.2.[72]

In the present study, the hydroxide-bound species $[M^{III}(PyPS)(OH)]^{2-}$ has been generated in solution by adjusting the pH of a solution of $[Fe^{III}(PyPS)(H_2O)]^-$ (in aqueous acetone) to 10. The same species is formed when $(Me_4N)(OH)$ is added to a solution of **1** in DMF/acetonitrile mixture. Binding of hydroxide ion to the iron(III) center of **1** results in low-spin $[M^{III}(PyPS)(OH)]^{2-}$ which exhibits a strong EPR signal with *g*-values = 2.22, 2.12, 1.99. The EPR spectrum (Figure 7) is comparable to the EPR spectrum of NHase (g = 2.21, 2.14, 1.95). These results support the notion that the water molecule bound at the iron center of NHase could exist as hydroxide at the functional pH of the enzyme (∼7.5), and hence such an iron center could hydrolyze substrates much like other known hydrolases.

Thermodynamics of Binding of Water and Pyridine to $(Et_4N)[Fe^{III}(PyPS)]$. These two ligands were chosen since they do not pose any effect due to charge and offer different donor atom (O vs N) to the iron(III) center of **1**. The van't Hoff plots for the binding of these two ligands (Figure S4) were used to calculate the enthalpy of formation (ΔH) of the adducts $[Fe^{III}(PyPS)(H_2O)]^-$ and $[Fe^{III}(PyPS)(py)]^-$. The ΔH value for the water adduct (−25.9 kcal mol^{-1}) is higher than that of the pyridine adduct (−21.3 kcal mol^{-1}), a fact that supports the higher affinity of the iron(III) center toward water, an O-donor. As mentioned before, binding of water is complete at −30 °C while for pyridine, complete binding is noted only at −70 °C. These results clearly indicate that the iron(III) center in **1** with coordinated carboxamido N and thiolato S donors prefers H_2O

(72) Sanchiz, J.; Dominguez, S.; Mederos, A.; Brito, F.; Arrieta, J. M. *Inorg. Chem.* **1997**, *36*, 4108.

Table 3. Electronic Absorption and EPR Data for the Six-coordinate Complexes

	λ_{max} (ϵ M^{-1} cm^{-1})[a]	*g* values[b]
$(Et_4N)[Fe^{III}(PyPS)(MeOH)]$	790 (950), 550 (3800), 410 (8500)	2.23 2.20 1.93[c]
$(Et_4N)_2[Fe^{III}(PyPS)(OH)]$	790 (700), 595 (3 900), 410 (7600)	2.31 2.12 1.93[d]
$(Et_4N)[Fe^{III}(PyPS)(N\text{-}MeIm)]$	910 (1600), 700 (1800), 420 (6500)	2.32 2.15 1.93[e]
$(Et_4N)_2[Fe^{III}(PyPS)(SPh)]$	640 (3400), 540 (4400)	2.27 2.13 1.96[f]
$(Et_4N)_2[Fe^{III}(PyPS)(CN)]$	910 (1800), 620 (2400)	2.30 2.11 1.96[g]
$(Et_4N)_2[Fe^{III}(PyPSO_2)(CN)]$	640 (1350), 470 (1600)	2.27 2.19 1.94[h]
$(Et_4N)_2[Fe^{III}(PyPSO_2)(CN)]$	660 (1200), 425 (1800)	2.20 1.93[h]

[a] See Experimental Section for details. [b] Spectra recorded at 77 K at X-band frequencies. Spectrometer settings: microwave frequency, 9.2 GHz; microwave power, 25 mW; modulation frequency, 100 kHz; modulation amplitude, 2 G. [c] MeOH glass of **1**. [d] $[Fe^{III}(PyPS)(OH)]^{2-}$ was generated as follows. 0.8 equiv of Me_4NOH was mixed with 1 equiv of **1** at 0 °C in a CH_3CN:DMF mixture and then frozen. [e] 1 equiv of N-MeIm was added to **1** in DMF and frozen. [f] 1 equiv of $(Et_4N)(SPh)$ added to **1** in DMF and frozen. [g] 1 equiv of $(Et_4N)(CN)$ to **1** in DMF and frozen. [h] DMF glass.

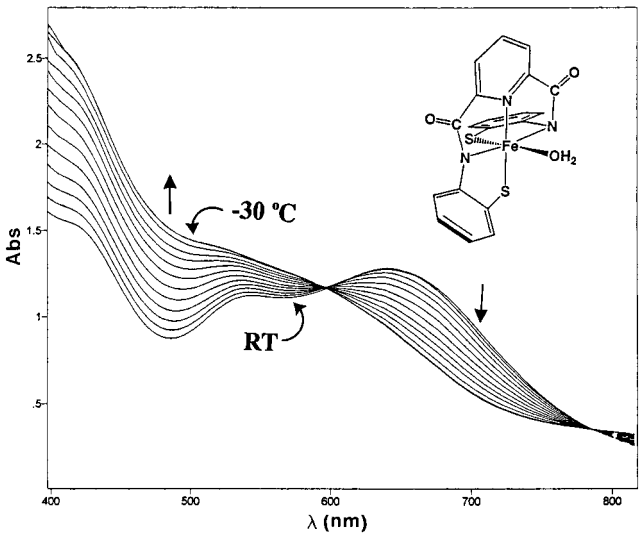

Figure 8. Top: Changes in the electronic absorption spectrum of a 0.35 mM solution of $[Fe^{III}(PyPS)]^-$ in acetone:water (30:70) mixture (pH 5.5) with temperature. At −30 °C, the final spectrum of the water adduct $[Fe^{III}(PyPS)(H_2O)]^-$ was recorded after 10 min.

over N-donors. Indeed, we did not notice any binding of nitriles to the iron(III) center of **1**. The suggestion that nitriles displace water bound to the iron(III) site in NHase and then are hydrolyzed thus appears to be unlikely.

Reactivity of $(Et_4N)[Fe^{III}(PyPS)]$ with Oxygen (O_2). One unique feature of the unprecedented coordination structure of the iron site in NHase is the presence of one sulfenato and one sulfinato group bound to the iron through the S centers. The oxidant responsible for the posttranslational modifications of the bound Cys-S donors at the active site of the enzyme is unknown at the present time. In the past, we have reported that iron(III) and cobalt(III) complexes that contain carboxamido N and thiolato S donors undergo oxidation of the ligated thiolato sulfurs to sufinates ($-\underline{S}O_2$) when reacted with H_2O_2.[49,50] In this work we show that the iron(III) complex **1** reacts readily with dioxygen to afford the corresponding sulfinato species $[Fe^{III}(PyP\{\underline{S}O_2\}_2)]^-$ (**2**) in which both the bound thiolato sulfurs are converted to sulfinato groups. To our knowledge, complex **1** is the first example of a model complex of NHase that shows this reactivity with dioxygen. Although Chottard and co-workers have reported a sulfinato species $(Et_4N)_2[Fe^{III}(L\text{-}O_2)]$ (structure ii), the corresponding thiolato complex is not reported, and the oxidant actually responsible for the thiolato → sulfinato transformation has not been identified.[45]

In contrast to the complex $(Et_4N)[Fe^{III}(PyPep\underline{S}O_2)_2]$ (structure v), where the sulfinato groups are coordinated to the iron(III) center via the sulfur atoms,[49] the sulfinato moieties of **2** undergo a structural rearrangement that results in the coordination of the oxygen atom of the sulfinato groups to the iron(III) center.

Scheme 1

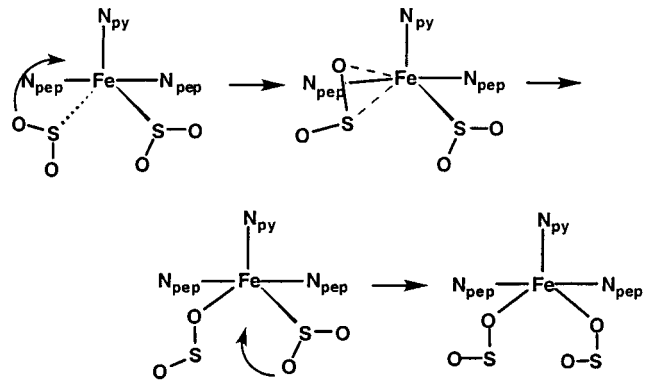

Affinity of iron(III) centers toward anionic oxygens could be the driving force for this rearrangement. It is interesting to note that oxidation of $(Et_4N)[Fe^{III}(PyPepS)_2]$ (structure iv) to $(Et_4N)[Fe^{III}(PyPep\underline{S}O_2)_2]$ does not allow such rearrangement. We attribute this difference in behavior to the coordinative saturation in $(Et_4N)[Fe^{III}(PyPepS)_2]$. For the rearrangement to take place, the O atom of the coordinated S-bonded sulfinato group should be temporarily ligated to the iron(III) center while the Fe−S bond starts to break (Scheme 1). Since $(Et_4N)[Fe^{III}(PyPepS)_2]$. does not have any such temporary site, oxidation of this complex results in pure $(Et_4N)[Fe^{III}(PyPep\underline{S}O_2)_2]$, the S-bonded sulfinato complex. In case of **1**, the iron(III) center is coordinatively unsaturated, and this fact allows temporary binding of the O-atom of the bound $-SO_2$ group to iron, and hence both the sulfinato groups sequentially isomerize to the O-bonded form (thermodynamically more stable) to afford **2** as the final product.

The reaction of **1** with dioxygen has been followed by electrospray mass spectrometry. As the solution of **1** in acetone is exposed to dioxygen, all intermediate oxygenated species with one, two, and three O atoms are observed along with $[Fe^{III}(PyP\{\underline{S}O_2\}_2)]^-$ (**2**) in the reaction mixture. It thus appears that the oxygenation reaction proceeds via a persulfoxidic intermediate which can give rise to products with bound sulfenato groups (i.e., products with one or three O atoms).[73−75] At the end of 48 h, only peaks corresponding to **2** are observed in the mass spectrum.

Addition of dilute hydrochloric acid to a solution of **2** in acetone removes the sulfinato ligand from iron as evidenced by the rapid loss of color. The precipitated ligand exhibits a single peak in the mass spectrum, corresponding to PyP-

(73) Grapperhaus, C. A.; Darensbourg, M. Y.; Sumner, L. W.; Russell, D. H. *J. Am. Chem. Soc.* **1996**, *118*, 1791.
(74) Farmer, P. J.; Solouki, T.; Soma, T.; Russell, D. H.; Darensbourg, M. Y. *Inorg. Chem.* **1993**, *32*, 4171.
(75) Farmer, P. J.; Solouki, T.; Mills, D. K.; Soma, T.; Russell, D. H.; Reibenspies, J. H.; Darensbourg, M. Y. *J. Am. Chem. Soc.* **1992**, *114*, 4601.

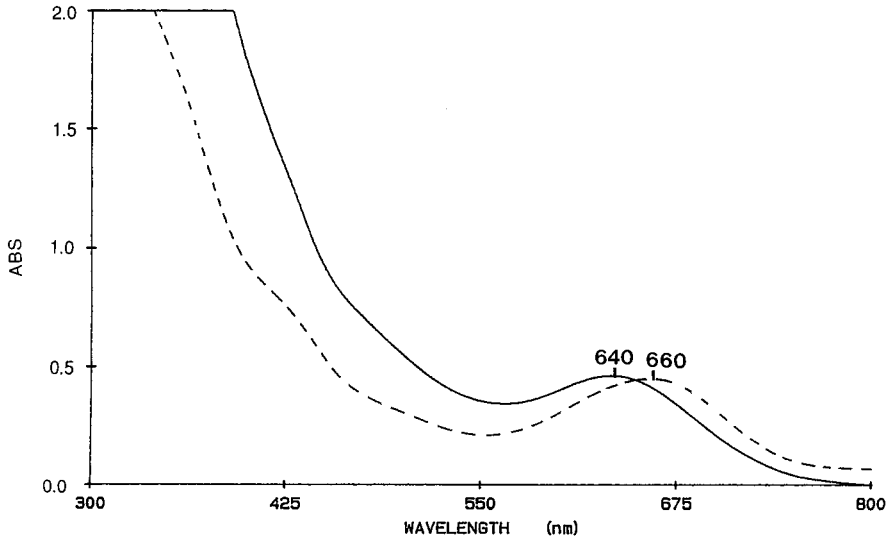

Figure 9. Electronic absorption spectra of $Na_2[Fe^{III}(PyP\{\underline{S}O_2)_2\})(CN)]$ (**4**) (solid line) and $(Et_4N)_2[Fe^{III}(PyP\{S\underline{O}_2)_2\})(CN)]$ (**5**) (broken line) in DMF (sample concentration: 0.4 mM).

$\{SO_2\}_2H_4$, and its IR spectrum displays strong ν_{NH} at 3271 cm^{-1}, ν_{CO} at 1656 cm^{-1}, and ν_{SO2} at 1121 and 1082 cm^{-1}. The deprotonated form of this ligand readily affords the iron(III) complex **2** in DMF. It thus appears that the preferred mode of binding of the sulfinato groups of $[PyP\{SO_2\}_2]^{4-}$ to iron(III) is through the O (not the S) atoms.

Reactivity of $(Et_4N)[Fe^{III}(PyPS)(CN)]$ with H_2O_2. In the previous section, we have hypothesized that the rearrangement of the S-bonded sulfinato complex to the O-bonded species can occur when the iron(III) center is not coordinatively saturated (Scheme 1). If this is true, then one expects to synthesize the S-bonded sulfinato complex via oxygenation of a coordinatively saturated iron(III) complex of $PyPSH_4$. Since we had access to such a complex, namely, $[Fe^{III}(PyPS)(CN)]^{2-}$, we studied the reactions of $[Fe^{III}(PyPS)(CN)]^{2-}$ with O_2 and H_2O_2. Although both reactions afforded the same results, the reaction with dioxygen was very slow. The reaction of $[Fe^{III}(PyPS)(CN)]^{2-}$ with H_2O_2 is, however, rapid even at subzero temperature and hence we have studied this reaction in detail. Reaction of H_2O_2 with $[Fe^{III}(PyPS)(CN)]^{2-}$ in acetonitrile at -20 °C affords $[Fe^{III}(PyP\{\underline{S}O_2\}_2)(CN)]^{2-}$ which has been isolated as the sodium salt and characterized by spectroscopic techniques, elemental analysis, and electrospray mass spectrometry. That the S atom of the sulfinato groups are bonded to the Fe(III) center in Na_2-$[Fe^{III}(PyP\{\underline{S}O_2\}_2)(CN)]$ (**4**) is evident from the similarities in spectroscopic parameters of this complex with those of the structurally characterized S-bonded sulfinato complex $Na[Fe^{III}$-$(PyPepSO_2)_2]$.[49] For example, the IR spectrum of **4** displays strong ν_{SO2} at 1186 cm^{-1}, while $Na[Fe^{III}(PyPep\underline{S}O_2)_2]$ exhibits ν_{SO2} at 1184 cm^{-1}. Dark-green solutions of **4** in water and DMF exhibit a moderately strong band with maximum at 670 and 640 nm, respectively. The EPR spectrum of **4** in DMF glass (g = 2.27, 2.19, 1.94) indicates the presence of a low-spin iron-(III) center (Figure S5, Supporting Information).

The spectral characteristics of the S-bonded sulfinato complex **4** are distinct from those of the O-bonded sulfinato complex $(Et_4N)_2[Fe^{III}(PyP\{S\underline{O}_2\}_2)(CN)]$ (**5**) which has been synthesized by the addition of CN^- to complex **2** in acetone. For example, the IR spectrum of **5** displays ν_{SO2} at 1030 cm^{-1}, a value close to the ν_{SO2} of **2** (1070 cm^{-1}), a O-bonded sulfinato complex. Also, in DMF, **5** exhibits an absorption band with maximum at 660 nm (Figure 9). The iron(III) center in **5** is also low-spin and gives rise to an axial EPR spectrum in DMF glass (g = 2.20, 1.93). Successful isolation of **4** and **5** provides support to our hypothesis that oxygenation of coordinatively saturated and kinetically inert iron(III) complexes gives rise to S-bonded sulfinato species.

Summary and Conclusions

The following are the principal results and conclusions of this investigation.

(i) The iron(III) and iron(II) complexes of a designed pentadentate ligand $PyPSH_4$ with two carboxamide and two thiolate groups have been synthesized and structurally characterized. These complexes add to the very short list of iron complexes that contain an iron(III) center ligated to deprotonated carboxamido nitrogens and thiolato sulfurs and are good structural models for the iron(III) site in Fe−NHase.

(ii) The redox potential of the iron(III) center in $(Et_4N)[Fe^{III}$-$(PyPS)]$ (**1**) (-0.65 V versus SCE in DMF) indicates that the carboxamido nitrogens provide significant stability to the +3 oxidation state of iron[76] and this in turn indicates that such stabilization could account for the absence of any redox activity of the iron site in NHase.

(iii) The coordinatively unsaturated iron(III) site in **1** binds various Lewis bases to give six-coordinate low-spin iron(III) species which afford green solution in water and DMF. Ligands such as methanol, water, pyridine, N-MeIm, and PhS^- bind at subzero temperature, while CN^- binds at room temperature. These results suggest that the low-spin green iron center in the enzyme is most probably six-coordinate.

(iv) The pK_a of the bound water molecule in $[Fe^{III}(PyPS)$-$(H_2O)]^-$ has been determined by low-temperature spectrophotometry. The pK_a value (6.3 ± 0.4) indicates that at physiological pH, the water at the iron(III) site in NHase could exist as hydroxide (as suggested by ENDOR studies on the enzyme). The pK_a of the bound water in the corresponding cobalt(III) complex $[Co^{III}(PyPS)(H_2O)]^-$ is 8.3, a fact that suggests that the iron-bound water is more acidic.

(v) The iron(III) center in **1** does not show any affinity toward nitriles even at low temperature. This behavior is observed with other model complexes. The enthalpy of formation of $[Fe^{III}$-$(PyPS)(H_2O)]^-$ (-25.9 kcal mol^{-1}) also indicates strong binding

(76) No oxidation wave corresponding to iron(III)/(IV) couple has been observed with **1** in any solvent up to +1.5 V (vs SCE).

by water and hence replacement of water (or hydroxide) at the active site of NHase by nitriles appears unlikely.

(vi) Exposure of solutions of **1** to dioxygen affords the O-bonded sulfinato complex $(Et_4N)[Fe^{III}(PyP\{S\underline{O}_2\}_2)]$ (**2**). This reaction mimics the posttranslational modification of the bound Cys-S centers of the active site of NHase. Conversion of similar thiolato complex $(Et_4N)[Fe^{III}(PyPepS)_2]$ to the S-bonded sulfinato complex $(Et_4N)[Fe^{III}(PyPep\underline{S}O_2)_2]$ indicates that the S-bonded iron(III) sulfinato species rearrange to the corresponding O-bonded species when the iron(III) center is coordinatively unsaturated (like $(Et_4N)[Fe^{III}(PyPS)]$). This is further supported by the fact that the coordinatively saturated complex $[Fe^{III}(PyPS)(CN)]^{2-}$ affords the S-bonded sulfinato complex $[Fe^{III}(PyP\{S\underline{O}_2\}_2)(CN)]^{2-}$ (**5**).

Acknowledgment. Financial support from NSF (CHE-9818492) and NIH (GM 61636) is gratefully acknowledged. J.C.N. received support from the NIH-IMSD Grant 1R25GM58903. The Bruker SMART 1000 diffractometer was funded in part by the NSF Instrumentation Grant CHE-9808259. We thank Dr. Robert Goldbeck and Dr. Trevor Swartz for experimental assistance.

Supporting Information Available: Crystal structure of complex **1** (Figure S1), electronic absorption spectrum of $(Et_4N)[Fe^{III}(PyPS)(N\text{-}MeIm)]$ in acetone at −70 °C (Figure S2), spectra of solutions of **1** in acetone:water mixtures at −30 °C vs the pH values (Figure S3), van't Hoff plots for binding of water and pyridine to the iron(III) center in **1** (Figure S4), EPR spectrum of complex **4** in DMF glass (Figure S5), crystal structure data for **1**−**3** including atomic coordinates and isotropic thermal parameters, bond distances and angles, anisotropic thermal parameters, and H-atom coordinates (PDF). This material is available free of charge via the Internet at http://pubs.acs.org.

JA001253V